

Microporous Mixed Octahedral-Pentahedral-Tetrahedral Framework Silicates

João Rocha and Zhi Lin

*Department of Chemistry, CICECO
University of Aveiro
3810-193 Aveiro, Portugal
rocha@dq.ua.pt*

INTRODUCTION

The frameworks of zeolites and related crystalline microporous oxide materials, such as aluminophosphates, silicoaluminophosphates and metaloaluminophosphates, are built up of tetrahedrally coordinated (e.g., Si, Al, P) atoms. Microporous structures comprised entirely of octahedral sites are also known, encompassing manganese oxides (OMS materials, Suib 1998) and phases with composition $\text{Na}_2\text{Nb}_{2-x}\text{M}_x\text{O}_{6-x}(\text{OH})_x \cdot \text{H}_2\text{O}$, where $M = \text{Ti}, \text{Zr}$, and $0 < x \leq 0.4$ (SOMS solids; Nyman et al. 2001, 2002). Mixed octahedral-pentahedral-tetrahedral microporous (OPT) siliceous frameworks have been much studied since the early 1990s (Rocha and Anderson 2000; Anderson and Rocha 2002). Comprehensive research into synthetic OPT materials was initiated by the seminal contributions of Kuznicki (1989, 1990) (titanosilicates ETS-4 and ETS-10), Chapman (1990); Chapman and Roe (1990) (ETS-4, and titanosilicate analogues of minerals vinogradovite and pharmacosiderite) and Anderson et al. (1994, 1995b) (ETS-10), and the early work of the groups of Raveau (Choisnet et al. 1976, 1977) (tantalo and niobosilicates), Corcoran and Vaughan (1989) and Corcoran et al. (1989, 1992) (stannosilicates).

Much research on the synthesis of OPT materials has been inspired and motivated by the many examples of such solids provided by Nature and brought to light by a plethora of mineralogists. As an example, consider the titanosilicate mineral zorite, discovered in 1973 on the Lovozero Tundra (Mer'kov et al. 1973). The structure solution of this mineral was published six years later by Sandomirskii and Belov (1979). Zorite is important because it was one of the first examples of microporous titanosilicates to be prepared in the laboratory (Kuznicki 1989; Chapman 1990; Chapman and Roe 1990). The details of the structure of the synthetic analogue of zorite, known as ETS-4, remained somewhat elusive until a single-crystal x-ray diffraction study published in 2001 settled the matter and clarified the differences between natural and synthetic materials (Nair et al. 2001). In the mean time, the desire to better understand the structure and properties of ETS-4 stimulated a considerable amount of work. The search for OPT silicates of metals other than titanium has also been guided by examples drawn from Nature. For instance, Bortun et al. (1997); Lin et al. (1999a,b); and Jale et al. (1999), extended the OPT field to zirconosilicates, reporting the synthesis of a synthetic analogue of the mineral gaidonnayite ($\text{Na}_2\text{ZrSi}_3\text{O}_9 \cdot 2\text{H}_2\text{O}$). Until the end of the last century, many microporous OPT minerals containing other metals, such as Nb, V, Sn and Ca, have been reported (Rocha and Anderson 2000; Anderson and Rocha 2002). Following the synthesis and structural characterization work, the potential applications of these novel materials have been evaluated, particularly in the areas of catalysis, separation and ion-exchange. It is appropriate to note here that, so far, most of this applied work concentrates on ETS-10 (more than 200 studies published) and, to a lesser extent, on ETS-4.

With the advent of the nanotechnology era, and the increasing interest in the use of molecular sieves for device applications (Tsapatsis 2002), the constituent elements of OPT materials have been further extended to the realm of lanthanide metals, exploring properties like photoluminescence (Rocha and Carlos 2003). In addition, at present, materials with interesting magnetic properties are also being sought after and this motivated, for example, the synthesis of copper silicates (Wang et al. 2003).

The field of zeolite membrane reactors has witnessed an intense research activity in the last ten years or so (Coronas and Santamaria 2004). However, as far as OPT materials are concerned, only a few studies are available on ETS-4 (Braunbarth et al. 2000a) and ETS-10 (Lin et al. 2004) membranes. Since the applications of molecular sieves in devices often require membranes, not powders, much work is now in progress in this area.

Advances in the field of OPT microporous materials have been reviewed by Rocha and Anderson (2000), Anderson and Rocha (2002) and Chukanov et al. (2004). Because significant progress has been made in the last three years, we believe it is now timely to appraise this recent work. Although clays and related materials, in some way, fall into the category of OPT materials, they only possess two-dimensional covalent connectivity and are out of the scope of this review. We concentrate on siliceous materials and, thus, overlook, for example, the important porous phosphates.

SYNTHESIS

Zeolites and OPT siliceous materials, particularly titanosilicates (Kuznicki 1989, 1990; Chapman 1990; Chapman and Roe 1990), are in general prepared under hydrothermal conditions, in Teflon-lined autoclaves, at temperatures ranging from *ca.* 120 to 230°C and times varying between a few hours and *ca.* 30 days. In a few cases, the hydrothermal synthesis was carried out at relatively high (e.g., 750°C) temperatures (Harrison et al 1995). For OPT materials, the pH of the synthesis gel is normally high, in the range 10–13 (after 1:100 dilution). Seeding the gel with a little amount of the desired phase (or even with a related solid) is a common practice. In general, stirring of the gel is not used, although a recent study of the synthesis of ETS-4 found that, under these conditions, the crystal morphology is quite different from that of materials prepared with no agitation. The syntheses are, in general, kinetically controlled, with different metastable phases being formed with time. Although most research has concentrated on the synthesis of microporous titanosilicates considerable experience has been gained into other systems, particularly, Zr, Nb, V and Sn silicates.

ETS-10 was first prepared by Kuznicki (1989), using TiCl_3 as the titanium source. A slight modification of this method afforded highly crystalline and pure ETS-10 suitable for structural investigation (Anderson et al. 1994, 1995b). TiCl_4 is another much used (and cheaper) titanium source (Das et al. 1996b) as is TiF_4 (Yang et al. 2001) a compound which has the advantage of not being sensitive to ambient air moisture. Anatase and rutile (TiO_2 phases, Liu and Thomas 1996) and $\text{Ti}(\text{SO}_4)_2$ (Kim et al. 2002) may also be used as suitable titanium sources for the synthesis of porous titanosilicates. The synthesis of ETS-10 has been carried out at 200°C using a 2^3 factorial method to optimize the overall composition of the reaction mixture to produce a pure material within a short (18 h) time. Kinetic studies on ETS-10 and ETS-4 have been performed using the optimum compositions and the apparent activation energies were calculated as 66.78 and 14.47 kJmol^{-1} , respectively (Kim et al. 2000). Thermodynamically, ETS-4 is more stable than ETS-10 with respect to the oxides (or the elements) at 298 K and 1 atm, probably because of the relatively higher degree of hydration of the former (Xu et al. 2001). This result has been obtained by high-temperature

drop solution calorimetry, which allowed the measurement of the pertinent standard enthalpies of formation from the oxides and from the elements.

A few organotitanium compounds, such as $\text{Ti}(\text{OC}_2\text{H}_5)_4$ (Chapman and Roe 1990) and titanium isopropoxide (Poojary et al. 1994) have also been used to prepare microporous titanosilicates. Because they are very sensitive to moisture, these compounds are difficult to handle and require special facilities for their transfer during the gel preparation. Sodium silicate solutions, fumed and colloidal silica are adequate silicon sources. Organosilicon compounds, such as tetraethylorthosilicate have also been used (Poojary et al. 1994). Although ETS-10 usually (although not always) crystallizes in the presence of Na^+ and K^+ ions, other phases, such as some of the AM-n (Aveiro-Manchester) microporous solids (Rocha et al. 1996a), are produced pure only when a single type of alkaline cation is present. Potassium fluoride is often used for preparing ETS-10 but its presence is not crucial. Comprehensive studies of the hydrothermal synthesis conditions, which yield pure and highly crystalline ETS-10 are now available (Rocha et al. 1998d; Das et al. 1995).

Although most OPT materials can be prepared without the addition of any organic templates, several groups have prepared ETS-10 with a range of templates: tetramethylammonium chloride (Valtchev and Mintova 1994; Valtchev 1994), pyrrolidine, tetraethylammonium chloride, tetrapropylammonium bromide, 1,2-diaminoethane (Valtchev 1994), choline chloride and the bromide salt of hexaethyl diquat-5 (Das et al. 1996a), ethanolamine (Kim et al. 2002). The latter work also reports kinetic studies, performed at different temperatures, where the interpretation of the data was carried out with a modified Avrami-Erofeev equation and the activation energies for nucleation, transition and crystal growth stages were calculated.

The framework substitution (doping) of titanium and silicon by other elements requires a judicious choice of the respective source which is usually introduced in the parent synthesis gel. The following sources of Al, Ga, Nb and B for element insertion in the ETS-10 framework have been reported: NaAlO_2 (Anderson et al. 1995a) GaCl_3 (Rocha et al. 1995) $\text{Nb}(\text{HC}_2\text{O}_4)_5$ (Rocha et al. 1999) and $\text{Na}_2\text{B}_2\text{O}_4$ (Rocha et al. 1998a; see also Kuznicki et al. 1991; Kuznicki and Trush 1991a, 1993). In the synthesis of microporous zirconosilicates ZrCl_4 (Jale et al. 1999; Rocha et al. 1998c; Lin et al. 1999a,b) and $\text{Zr}(\text{OC}_3\text{H}_7)_4$ (Bortun et al. 1997) have been used as the Zr sources, while the synthesis of lanthanide (Ln) silicates normally requires LnCl_3 or $\text{Ln}(\text{NO}_3)_3$ (Ananias et al. 2001).

A few authors have been devoting considerable attention to the study of the crystal growth mechanisms of ETS-4 and ETS-10. In view of the defect structures of these materials, this is a highly challenging task, which is increasing our understanding of the synthesis mechanisms of OPT materials and zeolites. Here we can only give a succinct outline of the subject. Miraglia et al. (2004) studied the hydrothermal synthesis of ETS-4 using organic precursors. The large, rectangular crystals and small, intergrown plates (cuboids), present were examined by AFM and FE-SEM, revealing a layered growth mechanism on the largest and slowest growing faces. These faces contain steps emanating from spiral hillocks with a characteristic height of one half of the orthorhombic ETS-4 unit cell parameter a . The disparity between the cuboid and rectangular crystal morphology indicates localized variations in Ti incorporation, nucleation and growth rate of ETS-4. Thus, to obtain uniform morphologies and minimize defects, solution chemistries need to be developed to improve miscibility and homogeneity. The group of Anderson has also much contributed for the elucidation of crystal growth mechanisms of zeolites (Anderson et al. 2001a,b). For example, they have shown that in ETS-10 the intergrowth structure and defects are also a consequence of a layer-by-layer growth mechanism which is described. With this knowledge of the crystal growth of ETS-10 strategies may now be developed to control the intergrowth structure and the defect density.

STRUCTURE

Titanosilicates

ETS-10 and ETS-4. ETS-10 and ETS-4 were prepared first at Engelhard Corporation (Kuznicki 1989, 1990). At about the same time Chapman (1990) and Chapman and Roe (1990), published the synthesis of a microporous titanosilicate material, whose structure apparently resembled the structure of the natural mineral zorite by comparison of the diffraction patterns. Owing to its wide-pore nature and thermal stability ETS-10 is the most important OPT microporous titanosilicate prepared so far. Because much has been written about the structure of ETS-10 and ETS-4, here we shall only summarize the main structural features of these materials.

The structure of ETS-10 $[(\text{Na,K})_2\text{Si}_5\text{TiO}_{13}\cdot x\text{H}_2\text{O}]$ was solved and reported briefly by Anderson et al. (1994) and later described fully by Anderson et al. (1995b) (Fig. 1). In 1999, a single crystal study of ETS-10 has refined the superposition structure, corresponding to an averaged combination of all the ordered variants, confirming substantially all previous structural work (Wang and Jacobson 1999). The structure comprises corner-sharing SiO_4 tetrahedra and TiO_6 octahedra linked through bridging oxygen atoms. The pore structure of ETS-10 contains 12-rings in all three dimensions; these are straight along $[100]$ and $[010]$ and crooked along the direction of disorder. Only a handful of microporous zeolitic materials with a three-dimensional 12-ring pore system are known and in this aspect ETS-10 has excellent diffusion characteristics. It is important to stress that the structure is inherently an intergrowth structure, consisting of randomly stacked layers. The basic unit is $\text{Si}_{40}\text{Ti}_8\text{O}_{104}^{16-}$ which is counterbalanced by 16 monovalent cations. Many ordered variants of ETS-10 exist, some of which are chiral (Fig. 1b). An important aspect of the structure of ETS-10 is that it contains $-\text{O}-\text{Ti}-\text{O}-\text{Ti}-\text{O}-$ chains (with alternating long-short bonds, according to Sankar et al. (1996) which are surrounded by a silicate ring structure. These combine to make up a rod and it is this rod nature which imparts ETS-10 some interesting physical properties. Adjacent layers of rods are stacked orthogonal to each other.

ETS-4 is essentially the synthetic analogue of the mineral zorite, possessing a mixed tetrahedral (Si)-pentahedral (Ti2)-octahedral (Ti1) framework (Sandomirskii and Belov 1979;

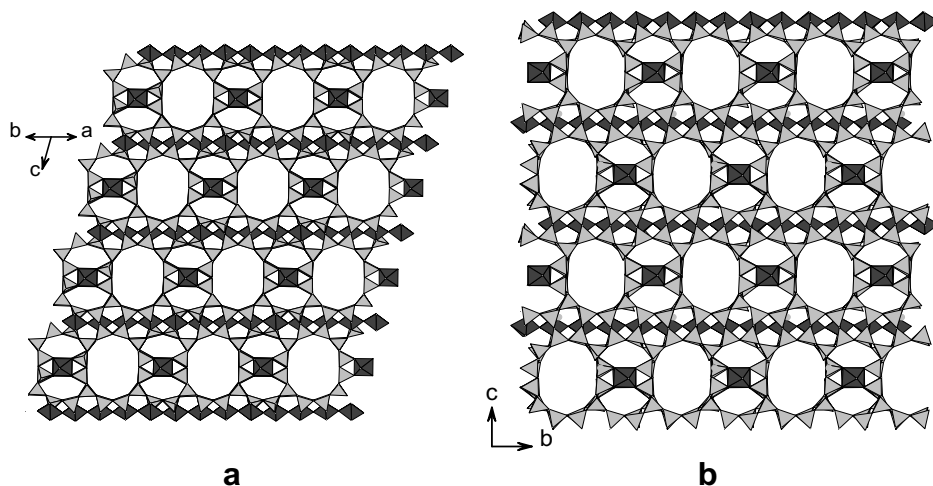


Figure 1. Titanosilicate ETS-10 projections: (a) down $[110]$ direction for polymorph B (space group $C2/c$); (b) down $[100]$ direction for polymorph A (space group $P4_1$). Dark TiO_6 octahedra, light grey SiO_4 tetrahedra.

Philippou and Anderson 1996; Cruciani et al. 1998, Braunbarth et al. 2000b; Nair et al. 2001). It is faulted in the [100] and [001] directions and can be described as a random intergrowth of four pure polytypes, which differ in the arrangement of the titanosilicate bridging units. Although larger openings are present in its structure, faulting ensures that access to the crystal interior of ETS-4 occurs through the relatively narrow 8-membered rings (Nair et al. 2001). A distinct feature of ETS-4 is the presence of semioctahedra (five-coordinated Ti with a titanyl, Ti=O, linkage to the apical oxygen) that are connected to framework silicon atoms through only four oxygen bridges, which gives rise to a planar connectivity. An intriguing difference between the structures of ETS-4 and zorite is the rotation of the TiO₅ square pyramid in zorite, an effect that is absent in ETS-4 for reasons which have been discussed (Nair et al. 2001). Kuznicki et al. (2001) have shown that the ETS-4 framework may be systematically contracted through dehydration at elevated temperatures to tune the effective size of the pores giving access to the crystal interior. This has been named 'molecular gate' effect and may be used to tailor the adsorption properties of the material to give size-selective adsorbents suitable for commercially important separations of gas mixtures of molecules with similar size in the 3.0–4.0 Å range, such as N₂/CH₄, Ar/O₂ and N₂/O₂. A pilot plant has been in use and successfully purified nitrogen contaminated natural gas by pressure swing adsorption at well-head pressures.

Recently, McDonald and Chao (2004) reported the structure of haineaultite, a new hydrated sodium calcium titanosilicate from Mont Saint-Hilaire (Quebec) with ideal formula (Na,Ca)₅Ca(Ti,Nb)₅(Si,S)₁₂O₃₄(OH,F)₈·5H₂O. The structure of this mineral consists of 8-rings of SiO₄ tetrahedra, linked to adjacent rings to form vierer double chains along [001], which are cross-linked by TiO₆ octahedra. Channels running parallel to [100] are occupied by Ca and H₂O, with Na residing in channels parallel to [001]. Haineaultite possesses an OD structure, exemplified by disordering of framework and interframework ions. The structures of haineaultite and zorite are similar. The main differences are: the species occupying the channels are not the same; the Ti polyhedra that cross-link the silicate chains are disordered TiO₅ polyhedra, in zorite, and ordered TiO₆ octahedra, in haineaultite. There are similarities between the crystal structure of haineaultite and mineral belonging to the rhodesite group (see the section on Rare-earth silicates), such as seidite-(Ce).

Like with conventional zeolites, the insertion of heteroatoms in the framework of OPT materials is an important process because it allows the fine-tuning of their properties (for example, substitution of Si by Al may generate sites for zeolite-type acidity). The studies on framework insertion of aluminum, gallium, boron, niobium, vanadium and chromium on ETS-10 and a few other materials have been reviewed (Rocha and Anderson 2000; Anderson and Rocha 2002).

Other titanosilicates. Although most research on OPT materials has been focused on ETS-4 and ETS-10, many other titanosilicate microporous materials are now known, most of which are synthetic counterparts of rare minerals. Importantly, these solids are in general small-pore silicates or tunnel structures, their porosity being only accessible to small molecules. As a result, the studies exploring their potential applications concentrate on ion-exchange properties.

Much has been learned from trying to mimic mineral pharmacosiderite, a non-aluminosilicate OPT molecular sieve with framework composition KFe₄(OH)₄(AsO₄)₃·6H₂O. Chapman and Roe (1990) prepared titanosilicate analogues of pharmacosiderite while, later, Behrens et al. (1996) studied in detail the structure of analogues with composition HM₃Ti₄O₄(SiO₄)₃·4H₂O, where M = H⁺, K⁺, Cs⁺. Harrison et al. (1995) grew single crystals of the same cesium phase and solved its structure by single-crystal methods. Pharmacosiderite materials possess a most interesting structure built up from TiO₆ octahedra sharing faces

to form Ti_4O_4 cubes placed at the corners of the cubic unit-cell; silicate tetrahedra join the titanium octahedra to form a three-dimensional framework. Extra-framework Cs^+ species occupy sites slightly displaced from the centers of the intercage eight-ring windows, and also make Cs-OH_2 bonds to the water molecules which reside in the spherical cages.

Poojary et al. (1994) reported the synthesis, crystal structure and ion-exchange properties of a novel porous titanosilicate of ideal composition $\text{Na}_2\text{Ti}_2\text{O}_3\text{SiO}_4 \cdot 2\text{H}_2\text{O}$ and whose structure is reminiscent of the structure of pharmacosiderite. The titanium atoms are octahedrally coordinated by oxygen atoms and occur in clusters of four, grouped about the 4_2 axis. The silicate groups link the titanium clusters into groups of four arranged in a square of about 7.8 Å in length. These squares are linked to similar squares in the c direction by sharing corners to form a framework enclosing a tunnel. Half the Na^+ ions are located in the framework, coordinated by silicate oxygen atoms and water molecules, while the remaining Na^+ ions reside in the cavity. The Na^+ ions within the tunnels are exchangeable, particularly by Cs^+ ions.

Another example of how the chemist draws lessons from Nature to engineer OPT materials is illustrated by the research carried out on the synthesis of analogues of nenadkevichite, a rare mineral first found in the Lovozero massif (Kola peninsula, Russia) and later in Mont Saint-Hilaire, Quebec (Canada), with the composition $(\text{Na,Ca})(\text{Nb,Ti})\text{Si}_2\text{O}_6(\text{O,OH}) \cdot 2\text{H}_2\text{O}$. Rocha et al. (1996a,b) prepared a series of synthetic analogues of nenadkevichite with Ti/Nb molar ratios ranging from 0.8 to 17.1 and a purely titaneous sample. The structure of nenadkevichite consists of square rings of silicon tetrahedra Si_4O_{12} in the (100) plane joined together by chains of $(\text{Nb,Ti})\text{O}_6$ octahedra in the [100] direction (Perrault et al. 1973). The pores accommodate Na^+ and water molecules.

Many porous framework titanosilicates contain Ti-O-Ti linkages which often form infinite chains. Interestingly, the materials known as AM-2 (Dadachov and Le Bail 1997; Lin et al. 1997, 1999a; Poojary et al. 1997; Jale et al. 1999), AM-3 and UND-1 (Liu et al. 1997a) do not contain any such linkages. AM-2 is a synthetic potassium titanosilicate analogue of the mineral umbite, a rare zirconosilicate found in the Khibiny alkaline massif, Kola Peninsula, Russia (Ilyushin 1993). Although the ideal formula of umbite is $\text{K}_2\text{ZrSi}_3\text{O}_9 \cdot \text{H}_2\text{O}$, a pronounced substitution of titanium for zirconium occurs. However, the natural occurrence of purely titaneous umbite is unknown. The successful synthesis of umbite materials with different levels of titanium for zirconium substitution has been reported (Lin et al. 1999b). AM-3 is the synthetic counterpart of the mineral penkvilksite, found at Mont Saint-Hilaire and Kola Peninsula, with formula $\text{Na}_4\text{Ti}_2\text{Si}_8\text{O}_{22} \cdot 5\text{H}_2\text{O}$. Penkvilksite occurs in two polytypic modifications, orthorhombic (penkvilksite-2O) and monoclinic (penkvilksite-1M), which have been described according to the OD theory as two of the four possible polytypes with the maximum degree of order within a family of OD structures formed by two OD layers (Merlino et al. 1994). Despite the different space group symmetries the 2O ($Pnca$) and 1M ($P2_1/c$) polytypes have the same atoms, labeled in the same way, in the asymmetric unit. They differ only in the stacking of the same building blocks. AM-3 is the synthetic analogue of penkvilksite-2O (Lin et al. 1997). The synthesis of the 1M polytype has been reported by Liu et al. (1997b, 1999). The material known as UND-1 ($\text{Na}_{2.7}\text{K}_{5.3}\text{Ti}_4\text{Si}_{12}\text{O}_{36} \cdot 4\text{H}_2\text{O}$) is the third example known of a porous framework titanosilicate containing *no* Ti-O-Ti linkages (Liu et al. 1997a).

A few other OPT titanosilicates, with a known structure, are available, for example the synthetic analogue of the mineral vinogradovite with composition $\text{Na}_5\text{Ti}_4\text{Si}_7\text{AlO}_{26} \cdot 3\text{H}_2\text{O}$ (Chapman and Roe 1990; Chapman 1990; Rastsvetaeva and Andrianov 1984). The structure of the mineral is composed of pyroxene chains joined to edge-sharing TiO_6 octahedra which form brookite columns. Vinogradovite chains $\text{Si}_3\text{AlO}_{10}$ consisting of four-membered rings connected through the common vertices are also involved in the framework of vinogradovite (the crystal structures of vinogradovite and related minerals are described in this volume by

Chukanov and Pekov 2005). These polyhedra define one-dimensional (4 Å free) channels containing zeolitic water. Examples of medium-size or large-pore titanosilicates whose structures are, as yet, unknown, have been reported (e.g., JLU-1 by Liu et al. 2000 and AM-18 by Brandão et al. 2002c).

A number of minerals not yet prepared in the laboratory exhibit very interesting and complexly connected frameworks (for a useful review see Smith 1988). A case in point is mineral verplanckite $[(\text{Mn}, \text{Ti}, \text{Fe})_6(\text{OH}, \text{O})_2(\text{Si}_4\text{O}_{12})_3]\text{Ba}_{12}\text{Cl}_9\{(\text{OH}, \text{H}_2\text{O})_7\}$, which has a framework with triple units of (Mn, Ti, Fe) in square-pyramidal coordination and four-rings of silicon tetrahedra (Kampf et al. 1973). The voids have a free diameter of 7 Å.

When attempting to prepare novel OPT titanosilicates, layered materials are sometimes obtained (e.g., AM-1, Anderson et al. 1995b; Lin et al. 1997, or JDF-L1, Du et al. 1996; Roberts et al. 1996, and AM-4 Lin et al. 1997; Dadachov et al. 1997), displaying interesting and unusual structures and presenting potential for being used in a number of applications such as ion exchange. An interesting future development in the OPT field is the synthesis of layered materials possessing microporous layers. These solids are of fundamental interest in exploring the connection between layered and framework silicates. An intriguing example is provided by Jeong et al. (2003) with a layered silicate known as AMH-3 ($\text{Na}_8\text{Sr}_8\text{Si}_{32}\text{O}_{76} \cdot 16\text{H}_2\text{O}$).

This material is composed of silicate layers containing 8-rings in all three principal crystal directions, and spaced by Sr^+ , Na^+ and water molecules. Nature is an endless source of inspiration: Krivovichev and Armbruster (2004) have recently reported the first example of a titanosilicate mineral (jonesite) with porous double layers (Fig. 2). The structure of jonesite, $\text{Ba}_2(\text{K}, \text{Na})[\text{Ti}_2(\text{Si}_5\text{Al})\text{O}_{18}(\text{H}_2\text{O})](\text{H}_2\text{O})_n$, from the Benitoite Gem Mine, San Benito County, California, is based upon porous double layers of distorted $\text{Ti}\Phi_6$ octahedra ($\Phi = \text{O}, \text{H}_2\text{O}$) and TO_4 tetrahedra ($T = \text{Si}, \text{Al}$) parallel to (010). The layers consist of two sheets of corner-sharing $\text{Ti}\Phi_6$ octahedra and Si_2O_7 groups each. The two adjacent sheets are linked along *b* by T_4O_{12} tetrahedral rings that are disordered over two positions. The double layer has an open structure characterized by 8-membered tetrahedral rings with free diameters of $3.37 \times 3.37 \text{ \AA}^2$ and $3.33 \times 3.33 \text{ \AA}^2$, for two symmetrically non-equivalent rings. K^+ and water molecules reside in the pores of the double layers. Ba^{2+} cations are located between the double layers and provide their linkage into a three-dimensional structure.

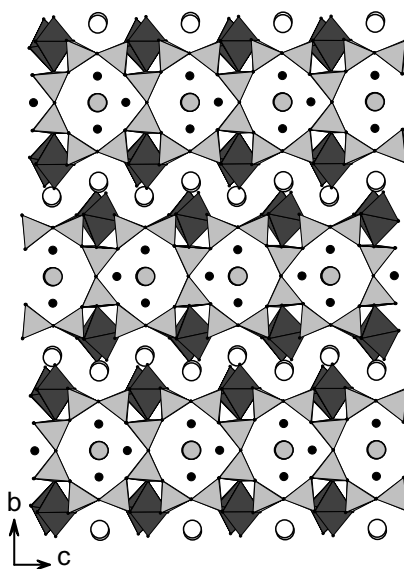


Figure 2. Crystal structure of jonesite: projection along the *a* axis showing the titanosilicate layers parallel to (010) with pores filled with (K,Na) and water molecules, linked by Ba. White circles Ba^{2+} ions, grey circles K^+ cations, dark circles H_2O .

Zirconosilicates

Zirconium silicates occur extensively in Nature. Their formation under hydrothermal conditions (from *ca.* 300 to 550°C) has been much studied, though mainly for the solution of general geophysical and mineralogical problems (Bortun et al. 1997). Maurice (1949) performed some of the first hydrothermal syntheses of zirconosilicates. Baussy et al. (1974)

summarized the early work in this field and report the hydrothermal synthesis of analogues of minerals such as catapleite ($\text{Na}_2\text{ZrSi}_3\text{O}_9 \cdot 2\text{H}_2\text{O}$) and elpidite ($\text{Na}_2\text{ZrSi}_6\text{O}_{15} \cdot 3\text{H}_2\text{O}$). Some interesting aspects of the chemistry of sodium zirconosilicates have been highlighted by the work of Bortun et al. (1997) reporting the synthesis, characterization and properties of three novel layered materials and five other zirconosilicates, for example a synthetic analogue of the mineral gaidonnayite ($\text{Na}_2\text{ZrSi}_3\text{O}_9 \cdot 2\text{H}_2\text{O}$). This material has also been synthesized by Lin et al. (1999a) (AV-4) and by Jale et al. (1999). The framework of gaidonnayite is composed of sinusoidal single chains of SiO_4 tetrahedra, repeating every six tetrahedra (Chao 1985). The chains extend alternately along [011] and $[\bar{0}1\bar{1}]$ and are cross-linked by a ZrO_6 octahedron and two distorted NaO_6 octahedra.

Petarasite [$\text{Na}_5\text{Zr}_2\text{Si}_6\text{O}_{18}(\text{Cl},\text{OH}) \cdot 2\text{H}_2\text{O}$] is another OPT zirconosilicate and its synthetic analogue is known as AV-3 (Lin et al. 1999a,b; Rocha et al. 1998c). The structure of this rare mineral is unusual, consisting of an open three-dimensional framework built of corner-sharing six-membered rings and ZrO_6 octahedra (Ghose et al. 1980). Elliptical channels ($3.5 \times 5.5 \text{ \AA}^2$) defined by mixed six-membered rings, consisting of pairs of SiO_4 tetrahedra linked by zirconium octahedra, run parallel to the *b* and *c* axes. Other channels limited by six-membered silicate rings run parallel to the *c* axis. The Na^+ , Cl^- , OH^- ions and the water molecules reside within the channels. The framework collapses only after the release of Cl at *ca.* 800°C.

Synthetic umbite-type materials have already been alluded to in this review. The synthesis and characterization of AV-8 ($\text{Na}_{0.2}\text{K}_{1.8}\text{ZrSi}_3\text{O}_9 \cdot \text{H}_2\text{O}$), an analogue of the mineral kostylevite, have been reported (Ferreira et al. 2001b). Kostylevite and umbite are the monoclinic and orthorhombic polymorphs of $\text{K}_2\text{ZrSi}_3\text{O}_9 \cdot \text{H}_2\text{O}$, respectively. The two minerals exhibit the same octagonal, heptagonal and hexagonal distorted tunnels and windows, delimited by edges from tetrahedra and octahedra alternating in exactly the same way. However, kostylevite is a cyclohexasilicate, while umbite is a long-chain polysilicate (Dadachov and Le Bail 1997). Titanosilicate UND-1 (Liu et al. 1997a) is a titanous analogue of kostylevite and, thus, also an analogue of AV-8. The thermal transformations of zirconosilicates AV-3 (synthetic petarasite) and AM-2 (analogue of umbite) yield analogues of the dense minerals parakeldyshite and wadeite, respectively.

Recently, Ferreira et al. (2003b) reported a small-pore zirconosilicate known as Zr-AV-13 ($\text{Na}_{2.29}\text{ZrSi}_3\text{O}_9\text{Cl}_{0.27} \cdot 2.5\text{H}_2\text{O}$) and tin and hafnium analogues of this solid. The structure of these materials is unprecedented, consisting of SiO_4 tetrahedra forming six-membered $[\text{Si}_6\text{O}_{18}]^{12-}$ rings which are interconnected by corner-sharing MO_6 ($M = \text{Zr}, \text{Hf}, \text{Sn}$) octahedra. The structure is better understood by considering a three-dimensional “knots-and-crosses” lattice. In a given layer, successive distorted-cube M_8 cages contain $[\text{Na}_{6-x}(\text{H}_2\text{O})_x](\text{H}_2\text{O},\text{Cl}^-)$ octahedral (knots) and cyclohexasilicate (crosses) units. While the former are extra-framework species, the 6-rings are part of the framework. The cages are accessed via seven-membered $[\text{M}_3\text{Si}_4\text{O}_{27}]^{26-}$ windows (free aperture $2.3 \times 3.3 \text{ \AA}^2$), one per each pseudo-cube face. Pilling up layers generates the structure, with knots-and-crosses alternating. This unusual structure shows that it is worth to further explore the chemistry of OPT zirconosilicates. Nature provides some interesting starting points for this endeavour. For example, mineral lemoynite, $(\text{Na},\text{K})_2\text{CaZr}_2\text{Si}_{10}\text{O}_{26} \cdot 5\text{--}6\text{H}_2\text{O}$, possesses a $\text{ZrSi}_5\text{O}_{13}$ framework with open channels where Na^+ , K^+ , Ca^{2+} and water molecules reside (Le Page and Perrault 1976). This framework comprises thick (7 Å) layers of hexagons of silicate groups. The sheets are bound together by six-coordinated zirconium atoms. The hexagons are tilted with respect to the (001) layer and the architecture of these layers is new. Another case in point is altsite, $\text{Na}_3\text{K}_6\text{Ti}_2[\text{Al}_2\text{Si}_8\text{O}_{26}]\text{Cl}_3$, an hyperalkaline aluminosilicate from the Kola Peninsula (Russia) related with lemoynite (Ferraris et al. 1995).

Vanadosilicates and niobosilicates

Some examples of OPT vanadosilicates have been reported (Evans 1973; Rinaldi et al. 1975; Rocha et al. 1997a; Wang et al. 2001, 2002c; Huang et al. 2002; Li et al. 2002). Among minerals, two solids stand out, cavansite and pentagonite, the dimorphs of $\text{Ca}(\text{VO})(\text{Si}_4\text{O}_{10})\cdot 4\text{H}_2\text{O}$. The tetrahedral layers consist of 6-rings in pentagonite and alternating 4- and 8-rings in cavansite, connected vertically by V(IV) cations in a square-pyramidal coordination (Evans 1973; Rinaldi et al. 1975). Replacement of the VO_5 groups by two bridging oxygens would produce a tetrahedral framework topologically identical to that of zeolite gismondine. The Ca^{2+} cations and the water molecules reside in the channels formed by the 8-rings and between the silicate layers. Cavansite has channels running parallel to the c direction with a free diameter of only 3.3 Å in the hydrated state. The first synthetic large-pore OPT vanadosilicate reported (AM-6) contains octahedral vanadium and possesses the structure of titanosilicate ETS-10 (Rocha et al. 1997a). The presence of stoichiometric amounts of vanadium in the framework of AM-6 affords this material potential for applications as a catalyst, sorbate or functional material.

The compelling work of Jacobson and co-workers (Wang et al. 2001, 2002c) shows that much remains to be learned in the field of OPT vanadosilicates: ten distinct framework types have been identified, all having structures based on cross-linking single silicate sheets with $\text{V}^{\text{IV}}\text{O}_5$ tetragonal pyramids or $(\text{H}_2\text{O})\text{-V}^{\text{IV}}\text{O}_5$ distorted octahedra, giving compounds with formula $A_x[(\text{VO})_b(\text{Si}_2\text{O}_5)_p(\text{SiO}_2)_q]_i\cdot \text{H}_2\text{O}$ ($A = \text{Na}, \text{K}, \text{Rb}, \text{Cs}$ or a combination). These, so-called, VSH- n structures have free channel diameters up to 6.5 Å and exhibit good thermal stability, absorption and ion-exchange properties. The structures of VSH-1K and VSH-2Cs are closely related to those of cavansite and pentagonite. Unlike other VSH- n materials which contain V(IV), VSH-16Na (Huang et al. 2002) is built up of $\text{V}^{\text{VI}}\text{O}_6$ octahedra which connect unbranched $[\text{Si}_8\text{O}_{22}]^{12-}$ chains (Fig. 3). Brandão et al. (2002a, 2003) reported several new large-pore vanadosilicates with unknown structure.

The structural diversity may be further expanded by substitution of the vanadyl groups with other components, such as $[\text{ZrF}_2]^{2+}$, $[\text{NbOF}]^{2+}$ and UO_2^{2+} (Wang et al. 2002c). For example, a series of uranium silicates have also been prepared by replacing the VO^{2+} cation in the vanadium(IV) silicates with UO_2^{2+} as the bridging metal species (Wang et al. 2002 a,b; Huang et al. 2003). The structures of USH- n , with $n = 2, 4, 5$, materials contain UO_6 tetragonal bipyramidal units connected by double chains, 4-rings and single chains of SiO_4 tetrahedra, respectively.

Comparatively few studies are available on OPT niobosilicates. The work carried out on nenadkevichite analogues containing titanium and niobium has already been mentioned in this review (Rocha et al. 1996a,b). The hydrothermal synthesis and evaluation of the catalytic properties of a microporous sodium niobosilicate whose structure is, at present, unknown have

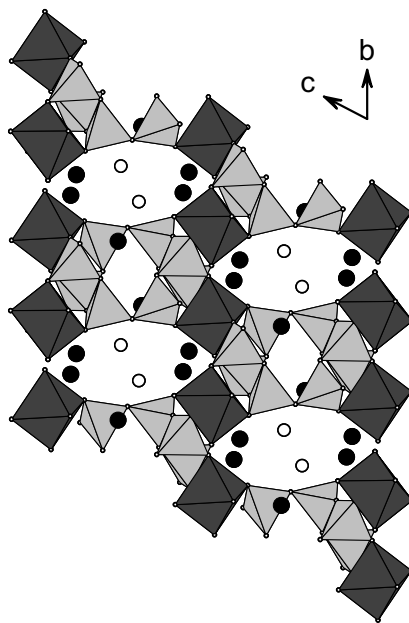


Figure 3. View of the structure of vanadosilicate VSH-16Na along [100]. Dark VO_6 octahedra, light grey SiO_4 tetrahedra, dark circles Na^+ cations, white circles H_2O .

been described (Rocha et al. 1998b; Philippou et al. 2001; Brandão et al. 2001a, 2002b). Francis and Jacobson (2001) reported the first organically templated OPT niobosilicate, $[(C_4N_2H_{11})Nb_3SiO_{10}]$ (NSH-1). The structure of this material is built up of two edge-shared NbO_6 octahedra that are further connected by corner-shared O atoms to form infinite double columns running along the $[010]$ direction (Fig. 4). A second chain of $[NbO_6-Si(Ge)O_4-NbO_6]_n$ polyhedra is formed from corner-sharing NbO_6 octahedra and runs along the $[100]$ direction. The two chains are cross-linked through O atoms to form the open-framework structure. The framework of NSH-1 consists of a network of three interconnecting one-dimensional channels, two consisting of 6-rings of polyhedra and the other an eight-membered ring. The two 6-ring channels are formed from six NbO_6 corner-linked units. The first runs along the $[100]$ direction; the second along the $[111]$ direction. The 8-ring channels are constructed from six NbO_6 and two SiO_4 units and run along the $[010]$ direction perpendicular to one of the 6-ring channels and at an angle of 55° to the other. The three channels intersect forming an irregular, roughly triangular shaped cavity, where the piperazinium cations reside. The 8-ring channels are elliptical in shape with an approximate free-pore diameter of $3.4 \times 5 \text{ \AA}^2$. Another interesting example of a niobosilicate, which is probably a tunnel structure, was reported recently (Kao and Lii 2002).

Stannosilicates and indosilicates

Although Dyer and Jáfar were probably the first authors to report the hydrothermal synthesis of an OPT stannosilicate (as a poster presented in 1987 at the Innovations in Zeolite Materials Science International Conference in Nieuwpoort, Belgium; pers. comm.), the early work in this field is due to Corcoran et al. (1989) and Corcoran and Vaughan (1989) carried out at Exxon Research. Some of these materials are useful sorbents, for example for the separation of hydrogen sulfides from gas streams containing hydrogen contaminated with hydrogen sulfides or oxysulfides (Corcoran et al. 1992). Later, Dyer and Jáfar (1990, 1991) also reported a microporous sodium stannosilicate and studied its ion-exchange properties for the replacement of Na^+ by a range of monovalent and divalent ions. However, the structures of all these materials have not been determined. Recently, we reported the synthesis and structures of microporous stannosilicates AV-6 and AV-7 analogues of, respectively, zirconosilicate minerals umbite (Lin et al. 1999b) and kostylevite (Lin et al. 2000). Two other materials were also

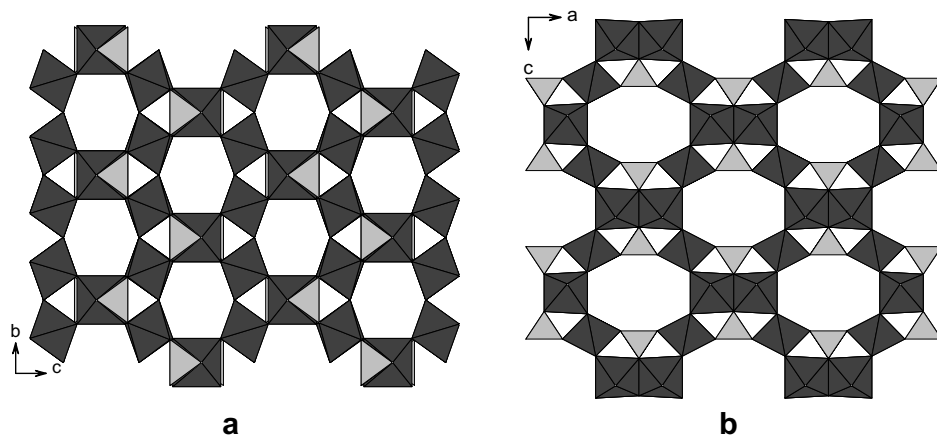


Figure 4. Structure of niobosilicate NSH-1 viewed (a) along the *a* axis, showing the 6-ring channels, and (b) along the *b* axis, showing the larger 8-ring channels. Dark NbO_6 octahedra, light grey SiO_4 tetrahedra. The template molecules are omitted for clarity.

reported, AV-10 (Ferreira et al. 2001a) and AV-13 (a tin analogue of the zirconosilicate AV-13 described above, Ferreira et al. 2003b). The powder XRD patterns of AV-6, AV-10 and AV-13 are similar to the patterns of, respectively, phases G, A and B reported by Corcoran et al. (1992). The very unusual structure of AV-10 (Ferreira et al. 2001a), $\text{Na}_2\text{SnSi}_3\text{O}_9 \cdot 2\text{H}_2\text{O}$ (chiral space group $C222_1$), is composed of corner sharing SnO_6 octahedra and SiO_4 tetrahedra, forming a three-dimensional framework structure (Fig. 5). The SiO_4 tetrahedra form helix chains along $[001]$ interconnected by SnO_6 octahedra. The SnO_6 octahedra are isolated by SiO_4 tetrahedra and, thus, there are no Sn-O-Sn linkages. The zeolitic water of AV-10 is reversibly lost.

Only a few examples of OPT indosilicates were reported and they were synthesized hydrothermally at high temperature (600°C) and pressure (170 MPa). For example, the structure of $\text{K}_2\text{In}(\text{OH})\text{Si}_4\text{O}_{10}$ consists of unbranched vierer 4-fold chains of corner-sharing SiO_4 tetrahedra running along the b axis linked together via corner sharing by chains of *trans*-corner-sharing $\text{InO}_4(\text{OH})_2$ octahedra to form a three-dimensional framework which delimits 8-ring and 6-ring channels to accommodate K^+ cations (Hung et al. 2003). Another case in point is $\text{Na}_5\text{InSi}_4\text{O}_{12}$ (Hung et al. 2004) isotypic with $\text{Na}_5\text{ScSi}_4\text{O}_{12}$ (Merinov et al. 1980). The structure consists of 12-membered single rings of corner-sharing SiO_4 tetrahedra linked together via corner sharing by single InO_6 octahedra to form a three-dimensional framework delimiting two types of channels along the c -axis. Two types of Na^+ ions are present: those within the 12-ring channels are immobile while the Na^+ ions within 7-ring channels are highly mobile.

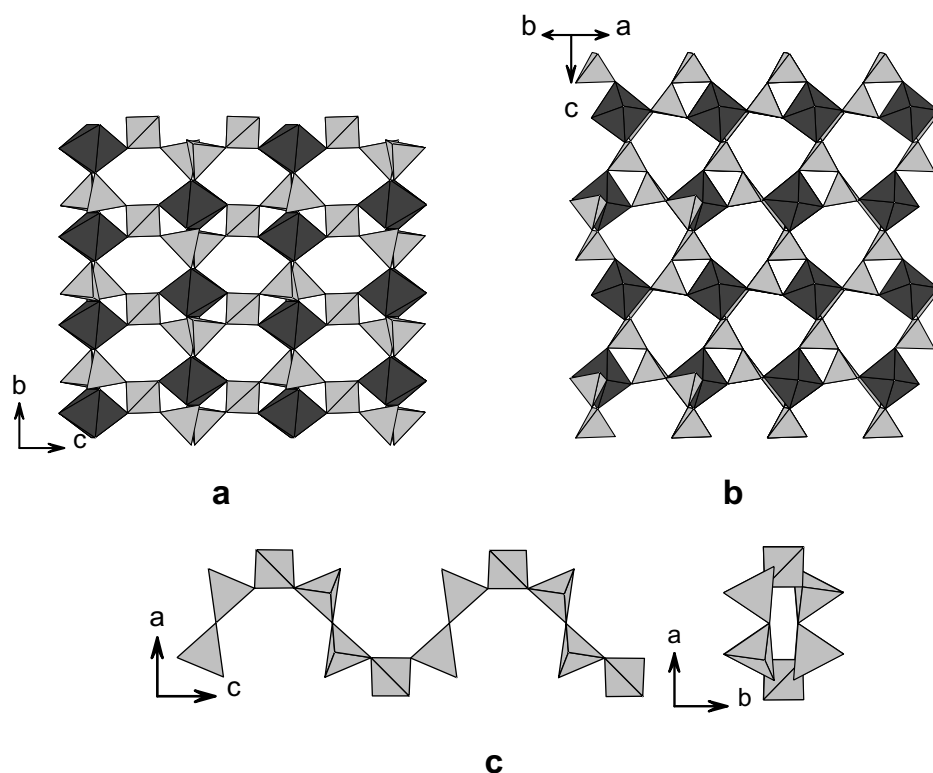


Figure 5. (a,b) Polyhedral representation of the structure of stannosilicate AV-10; (c) the helix chains of SiO_4 tetrahedra in AV-10. Dark SnO_6 octahedra, light grey SiO_4 tetrahedra. Cations and water molecules are omitted for clarity.

Rare-earth silicates

Research into OPT rare-earth silicates is, at present, a very active field of research because the presence of lanthanide ions affords the materials interesting photoluminescence properties. As an example, consider AV-1 ($\text{Na}_4\text{K}_2\text{Y}_2\text{Si}_{16}\text{O}_{38}\cdot 10\text{H}_2\text{O}$), the synthetic analogue of the rare mineral monteregianite-(Y) (Rocha et al. 1997b; Rocha et al. 1998e). This yttrium silicate possesses an unusual structure (Fig. 6) consisting of two different types of layers alternating along the [010] direction (Ghose et al. 1987): (a) a double silicate sheet, where the single silicate sheet is of the apophyllite type with 4- and 8- rings, and (b) an open octahedral sheet composed of YO_6 and three distinct $[\text{NaO}_4(\text{H}_2\text{O})_2]$ octahedra. The layers are parallel to the (010) plane. The K^+ ions are ten-coordinate and the six water molecules are located within large channels formed by the planar eight-membered silicate rings. The structure of the alkali calcium silicate mineral rhodesite, $\text{HKCa}_2\text{Si}_8\text{O}_{19}\cdot 6\text{H}_2\text{O}$ (Hesse et al. 1992) and its synthetic analogue AV-2 (Rocha et al. 2000b) is closely related to that of monteregianite. Rhodesite and monteregianite-(Y) have double silicate layers of the same topology. In fact, other minerals such as delhayelite, hydrodelhayelite and macdonaldite, all have similar double silicate sheets. In rhodesite, these layers possess the maximum topological symmetry ($P2mm$) while in monteregianite-(Y) symmetry has been lost.

Rocha et al. (2000b) reported the first microporous sodium cerium silicate (AV-5) possessing the structure of mineral monteregianite-(Y). Recently, the same group reported the synthesis and *ab initio* structure determination of the first sodium potassium microporous

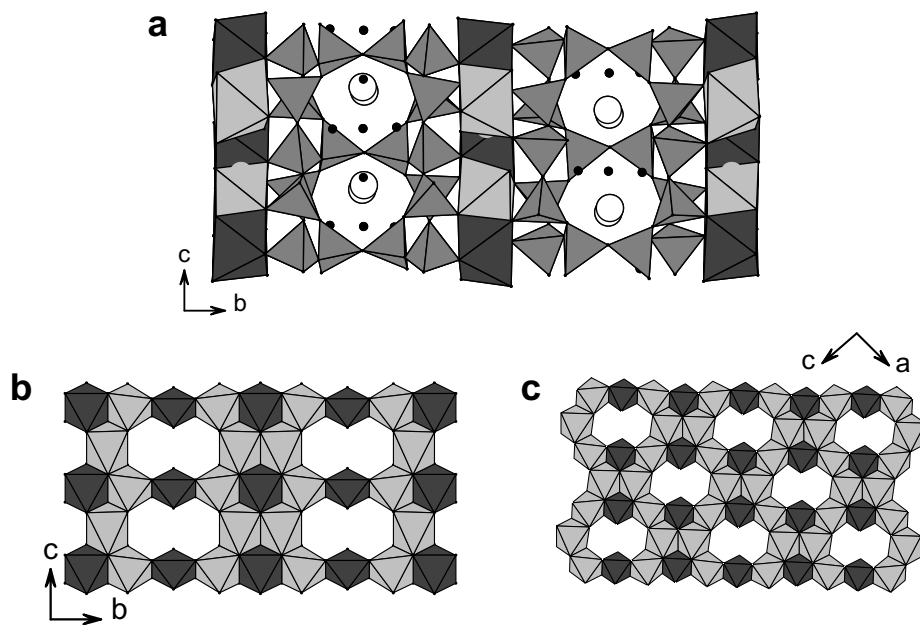


Figure 6. (a) Crystal structure of monteregianite-type materials showing two types of alternating layers: a double silicate sheet, and (b,c) an open octahedral sheet composed of LnO_6 and $[\text{NaO}_4(\text{H}_2\text{O})_2]$ octahedra. The tetrahedral layers of all these solids are similar but this is not the case with the octahedral layers. For example, monteregianite and its Y^{3+} and Ce^{3+} analogues contain a single type of Ln^{3+} facing the pores (c), while the Eu^{3+} and Tb^{3+} analogues contain two types of Ln^{3+} , one is isolated by $[\text{NaO}_4(\text{H}_2\text{O})_2]$ octahedra and the other faces the pores (b). Dark LnO_6 octahedra, light grey $[\text{NaO}_4(\text{H}_2\text{O})_2]$ octahedra, medium grey SiO_4 tetrahedra, white circles K^+ ions, dark circle H_2O .

europium and terbium silicates, named AV-9 (Ananias et al. 2001). The structures of AV-9 materials (and related materials containing Er, Tb, Ananias et al. 2004, and Nd, Rocha et al. 2004a) and mineral monteregianite-(Y) are related. However, although the tetrahedral layers of AV-9 solids and monteregianite-(Y) are similar this is not the case with the octahedral layers. Perhaps the most important difference between the octahedral layers of AV-9 and monteregianite lies in the fact that the latter contains a single kind of Y(III), facing the pores, while AV-9 contains two kinds of Eu(III), Tb(III): one is isolated by $[\text{NaO}_4(\text{H}_2\text{O})_2]$ octahedra while the other is facing the pores. This is expected to influence, for example, the luminescence behavior of these two Eu(III), Tb(III) centers. Rhodesite-type minerals are also discussed by Ferraris and Gula (2005) in this volume.

Another interesting system, is based on mineral sazhinite-(Ce) $\text{Na}_2(\text{CeSi}_6\text{O}_{14})(\text{OH}) \cdot 1.5\text{H}_2\text{O}$ (Shumyatskaya et al. 1980). For example, AV-21 $[\text{Na}_3(\text{EuSi}_6\text{O}_{15}) \cdot 2\text{H}_2\text{O}]$ contains two crystallographically distinct Eu^{3+} centers coordinated to six different SiO_4 tetrahedra, in a distorted octahedral coordination (Rocha et al. 2004b). The crystal structures of AV-21, cerium silicate $\text{Na}_3(\text{CeSi}_6\text{O}_{15}) \cdot 2\text{H}_2\text{O}$ recently reported by Jeong et al. (2002a), mineral sazhinite-(Ce), and the α and β forms of $\text{K}_3(\text{NdSi}_6\text{O}_{15}) \cdot x\text{H}_2\text{O}$ (Haile and Wuensch 2000a,b) show several remarkable similarities. All structures are formed by undulated $[\text{Si}_2\text{O}_5]_{\infty}^{2-}$ layers (in the bc plane, for AV-21, Fig. 7b) in which all the SiO_4 tetrahedra are formed by three bridging O-atoms (to neighboring intra-layer Si-atoms) and one terminal O-atom coordinated to one Eu^{3+} ion (tetrahedral vertices pointing “upwards” and “downwards” in Fig. 7). Although in all the structures the layers are formed by the condensation of adjacent xonotlite-type ribbons the way they coalesce in AV-21 and $\text{Na}_3(\text{CeSi}_6\text{O}_{15}) \cdot 2\text{H}_2\text{O}$ is different from what is observed for

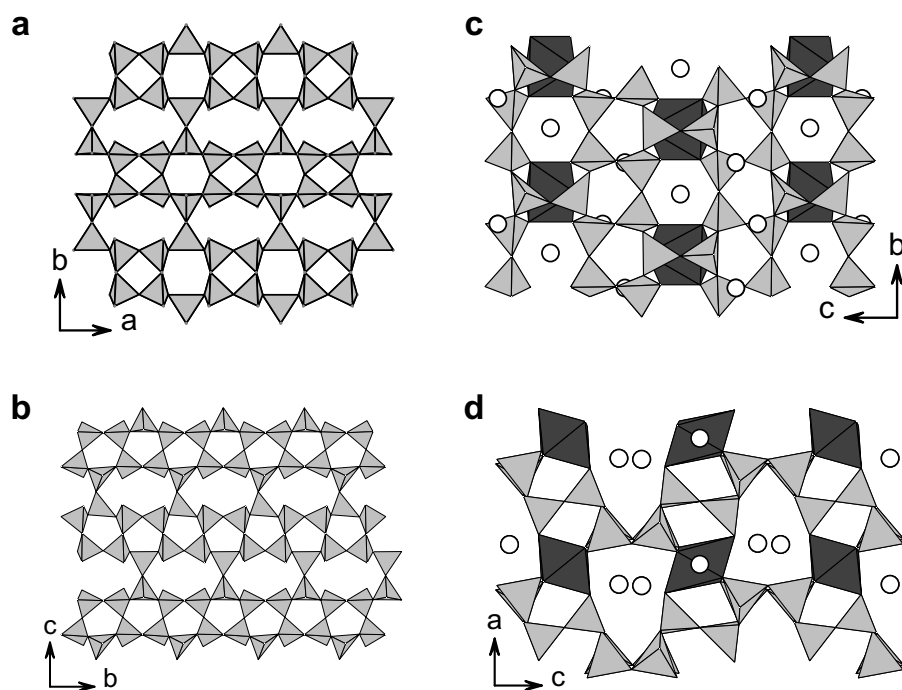


Figure 7. $[\text{Si}_2\text{O}_5]_{\infty}^{2-}$ layers present in (a) mineral sazhinite-(Ce) [and in the α and β forms of $\text{K}_3(\text{NdSi}_6\text{O}_{15}) \cdot x\text{H}_2\text{O}$] and (b) sodium europium silicate AV-21 [similar to layers in $\text{Na}_3(\text{CeSi}_6\text{O}_{15}) \cdot 2\text{H}_2\text{O}$]. (c,d) Polyhedral representation of the structure of AV-21.

sazhinite and the α and β forms of $\text{K}_3(\text{NdSi}_6\text{O}_{15}) \cdot x\text{H}_2\text{O}$: while in the mineral (and related structures) the coalescence of xonotlite-type ribbons leads to the formation of alternating 4- and 6-rings in the interface between ribbons (Fig. 7a), for AV-21 and $\text{Na}_3(\text{CeSi}_6\text{O}_{15}) \cdot 2\text{H}_2\text{O}$ only 5-rings are observed in the interface due to an alternate way of connection, with relative shift of adjacent xonotlite ribbons (Fig. 7b). Adjacent $[\text{Si}_2\text{O}_5^{2-}]_\infty$ layers are pillared by the Eu^{3+} ions, connected through coordinative interactions to the terminal SiO_4 oxygen atoms, forming a porous three-dimensional network (Fig. 7c,d). Sazhinite-(Ce) contains channels running along each crystallographic direction of the unit cell. The largest channels are formed by the hills and valleys of the corrugated $[\text{Si}_2\text{O}_5^{2-}]_\infty$ sheets, which leads to the formation of two different types of irregular 8-membered tunnels (cross-sections of *ca.* $4.2 \times 3.2 \text{ \AA}^2$ and *ca.* $3.0 \times 2.0 \text{ \AA}^2$ for the channels which contain water molecules and Na^+ , respectively) (Shumyatskaya et al. 1980). The same structural type of 8-membered channel is also observed for AV-21 (running parallel to the *b* axis with cross-section of *ca.* $3.0 \times 1.8 \text{ \AA}^2$; Fig. 7d), $\text{Na}_3(\text{CeSi}_6\text{O}_{15}) \cdot 2\text{H}_2\text{O}$, and the α and β forms of $\text{K}_3(\text{NdSi}_6\text{O}_{15}) \cdot x\text{H}_2\text{O}$. It is interesting to note that in these compounds only one type of channel is observed, with shapes best described as intermediate between the shapes of the two different channels present in sazhinite-(Ce). In AV-21 and $\text{Na}_3(\text{CeSi}_6\text{O}_{15}) \cdot 2\text{H}_2\text{O}$, the alternate way for the xonotlite-type ribbons in the $[\text{Si}_2\text{O}_5^{2-}]_\infty$ layers also has the peculiar feature of forming channels only in two crystallographic directions of the unit cell (in AV-21, channels are present along the *a* and *b* axes, Fig. 7c,d). Na^+ ions and water molecules are located within the channels of the open anionic frameworks.

A common feature of the tobermorite (hydrated calcium silicates) mineral family is the layer built up by seven-coordinated (mono-capped trigonal prisms) calcium cations, as described by Bonaccorsi and Merlino (2005) in this volume. Tobermorites are, thus, not OPT materials but they deserve a reference here because the interesting photoluminescence properties of AV-20 materials (Ferreira et al. 2003a) and the rare-earth OPT silicates described above are somewhat similar. The structure of Eu-AV-20 is closely related with the structure of tobermorite 11 \AA minerals. In AV-20, the substitution $2 \text{Ca}^{2+} \leftrightarrow \text{Eu}^{3+} + \text{Na}^+$ occurs, with Eu^{3+} and Na^+ being seven-coordinated. In addition, some (*ca.* 10%) Eu^{3+} ions are disordered over the Na^+ sites. Other lanthanide ions may be introduced into the structure.

PROPERTIES AND APPLICATIONS

Catalysis and sorption

So much work is now available on the evaluation of the catalytic properties of ETS-10 and related materials (and to some extent on ETS-4) that here only some key features will be highlighted. The catalytic applications have focused on the following attributes of ETS-10: high cation exchange capacity leading to many possibilities particularly in base catalysis; facile metal loading for bi-functionality; very low acidity; possible chiral activity; photocatalytic properties. On the other hand, the titanosilicates with octahedrally-coordinated titanium do not show good properties for oxidation catalysis in a similar manner to four-coordinate titanium. This is due to the ligand saturation which prevents further attachment by oxidation agents such as hydrogen peroxide.

At present, the study of the photo-reactivity of ETS-10 (Howe and Krisnandi 2001) and the evaluation of this material in photo-catalysis (Calza et al. 2001) is an area of intense research. For example, the activity of ETS-10 for the photo-catalytic degradation of cyclohexanol, cyclododecanol, 2-hexanol, and benzyl alcohol was compared with TiO_2 particles included within small and large pore zeolitic supports suspended in acetonitrile by Fox et al. (1994). Southon and Howe (2002) reported that the disordered stacking of repeat units in the structure of ETS-10 gives rise to defects that strongly influence the reactivity. Changes in the ultra-

violet absorbance spectrum indicated disruptions of the delocalized charge-transfer transitions along the -Ti-O-Ti- chains. The stacking defects interrupt these chains and hydroxyl groups are associated with these defects. The same group later reported that the photo-reactivity and photo-catalytic activity of ETS-10 are strongly influenced by the defects in the structure (Krisnandi et al. 2003). A relatively defect free material catalyses the photo-polymerization of ethane and in the presence of oxygen catalyses the partial oxidation of ethene to acetic acid and acetaldehyde, which remain strongly adsorbed in the pores. A more defective material is photo-reduced when irradiated in the presence of adsorbed ethene, and catalyses the complete oxidation of ethene to carbon dioxide and water in the presence of oxygen. Although Calza et al. (2001) have shown that ETS-10 can be used as a shape-selective photocatalyst for the decomposition of aromatic molecules, the actual use of this material is discouraged by its low activity, when compared with that of TiO_2 . Later, the same group showed that a mild treatment with HF enhances the activity of ETS-10 in the photo-degradation of large aromatic molecules that are unable to penetrate inside the pores, such as 2,5-dichlorophenol, 2,4,5-trichlorophenol, 1,3,5-trihydroxybenzene, and 2,3-dihydroxynaphthalene (Xamena et al. 2003). The photo-activity of the acid-treated materials is comparable to, or greater than, that of the nonselective TiO_2 catalyst. Moreover, the enhancement of the photoactivity is accompanied by a parallel increase of the shape selectivity, particularly toward dihydroxynaphthalene. Uma et al. (2004) explored the photo-catalytic decomposition of acetaldehyde over ETS-10 and transition metal ion exchanged ETS-10 decomposed acetaldehyde under UV radiation and the rate constant for the decrease of acetaldehyde is comparable to that of pure TiO_2 . Interesting visible ($\lambda > 420 \text{ nm}$) and UV light activity was found for ETS-10 samples incorporated with Cr and Co (Cr, Co/Ti = 0.05) and for materials synthesized by ion-exchange reactions such as Co-ETS-10 and Ag-ETS-10. All other ion-exchanged $(\text{Na,K})_{(2-x)}\text{M}'_x\text{TiSi}_5\text{O}_{13}$ [$\text{M}' = \text{Cr(III)}$, Mn(II) , Fe(III) , Co(II) , Ni(II) , and Cu(II)] samples were found to be active photo-catalysts that can decompose acetaldehyde under UV radiation. So far, the photo-catalytic activity of ETS-4 deserved much less attention. A recent study by Guan et al. (2004) explored a CdS/ETS-4 composite for hydrogen production from water under visible light irradiation ($\lambda > 420 \text{ nm}$). It was found that nano-sized CdS particles embedded in the ETS-4 nano-pores show stable photo-catalytic activity in an aqueous solution containing Na_2S and Na_2SO_3 electron donors and the energy conversion efficiency was improved by combining CdS with ETS-4.

Bianchi and Ragaini 1997; Bianchi et al. (1996, 1998a,b) report on Fischer-Tropsch chemistry over Co and Ru exchanged ETS-10. This material was found to be a suitable support for metal catalysts, having high surface area, high ion-exchange capability and no acidic function. The importance of alpha-olefin readsorption within the catalyst is discussed and the nature of this readsorption is tailored by effective control of the metal distribution inside the pores of ETS-10. The CO conversion and selectivity obtained also varies depending upon whether the active metal is introduced in the ETS-10 cages by ion-exchange or simply by impregnation.

Philippou et al. (1998a), Waghmode et al. (1999) and Das et al. (1997, 1998) have studied the bifunctional reforming reaction of hexane to benzene over Pt-supported basic ETS-10. The basicity of the titanosilicate can be controlled through samples exchanged with different alkali metals ($M = \text{Li}$, Na , K , Rb , or Cs). A distinct relationship between the intermediate electronegativity (S-int) of the different metal-exchanged ETS-10 samples and benzene yield is reported, suggesting the activation of Pt by the basicity of the exchanged metal. ETS-10 samples exhibit greater aromatization activities than related $\text{Pt-Al}_2\text{O}_3$ catalysts. The very high basicity of ETS-10 in comparison with, for example zeolite X, is illustrated by Philippou et al. (1999) in a paper which monitors the relative conversion of isopropanol to acetone. The same group has also demonstrated how these same properties are effective in aldol chemistry (Philippou and Anderson 2000) and dehydration of *t*-butanol (Philippou et al. 1998b;

Das et al. 1996c). In this latter reaction conversions and selectivities close to 100% are observed at relatively modest temperatures.

Acylation of alcohols with acetic acid can be carried out efficiently in the liquid phase over ETS-10 exchanged with several ions (Waghmode et al. 2001). The best activity for acylation of primary alcohols is found for H, Rb and Cs-ETS-10. ETS-10 may also be used for the acylation of secondary alcohols and esterification with long chain carboxylic acids.

Pd-loaded ETS-10 was used as a catalyst in Heck reaction (Waghmode et al. 2003). The catalyst exhibits high activity and selectivity towards the carbon-carbon coupling of aryl halides with olefins. In the case of the coupling of ethyl acrylate with iodobenzene, 96% conversion of iodobenzene with greater than 98% selectivity was obtained within one hour over a 0.2 wt% Pd-loaded catalyst. The catalyst activates aryl bromide and chloride substrates, and appears to be heterogeneous.

ETS-10 was shown to be a good catalyst for the transesterification of soybean oil with methanol, providing higher conversions than zeolite X (Suppes et al. 2004). The increased conversions were attributed to the higher basicity of ETS-10 and larger pore structure that improved intra-particle diffusion.

The catalytic activity of a series of Cr-containing ETS-10 samples with different Cr/Ti was characterized by standard probe reactions (Brandão et al. 2001b): isopropanol conversion (to propene and acetone), *t*-butanol conversion (to iso-butene) and ethanol oxidation (to acetaldehyde and ethyl acetate).

The gas-phase oxidative dehydrogenation of cyclohexanol with air using ETS-10 materials has been studied (Valente et al. 2001). At reaction temperatures below 200°C ETS-10 is 100% selective to cyclohexanone and 75% cyclohexanol conversion is achieved. The introduction of Cr, Fe and K, Cs in ETS-10 changes the stability and decreases the conversion and selectivity towards cyclohexanone.

The de-NO_x activity of Cu-based catalysts prepared by dispersing CuO on ETS-10 was studied by Gervasini and Carniti (2002). The activity of NO reduction with ethylene was related to the morphological and chemical properties of the catalysts. The results are consistent with a value of about 2.5–3 atom(Cu) nm⁻² for the maximum dispersion capacity of CuO on the ETS-10 matrix. The amount of Cu deposited on ETS-10 affects the activity of catalysts towards NO reduction. The turnover frequencies per Cu site calculated as a function of Cu concentration showed a clear decreasing trend starting from 0.7 to 3.5 atom(Cu) nm⁻².

Bal et al. (2000) carried out an EPR study of Ti(III) in ETS-4, ETS-10, TS-1 and TiMCM-41. Ti(III) was obtained by reduction of Ti(IV) by dry hydrogen at temperatures above 673 K. Interaction of tetrahedrally-coordinated Ti(III) (in TS-1 and TiMCM-41) with O₂ and H₂O₂ results in a diamagnetic Ti(IV) hydroperoxo species. Under the same conditions, octahedrally-coordinated Ti(III) (in ETS-4 and ETS-10) forms a paramagnetic Ti superoxo species. The poor activity in selective oxidation reactions of ETS materials has been attributed to the absence of formation of titanium hydroperoxo species.

Bodoardo et al. (2000) studied the status of Ti(IV) in ETS-10 and TS-1 by voltammetry. Both, tetrahedral and octahedral, TS-1 Ti(IV) species show electrochemical response. It was shown that the use of acid solutions allows discrimination between Ti(IV) ions in TS-1 and in ETS-10, since only the former is able to coordinate water molecules.

Zecchina et al. (2001) investigated the interaction of methyl and ethyl acetylene with the acidic form of ETS-10. In the first adsorption step, at room temperature, π hydrogen-bonded adducts are formed between the alkyl acetylene and ETS-10 hydroxyl groups. These hydrogen-

bonded species act as precursors in the second step where oligomerization takes place, leading to formation of carbocationic double-bond conjugated systems of increasing length. The same group also reported on the adsorption of carbon dioxide on Na- and Mg-exchanged ETS-10 (Xamena and Zecchina 2002). CO₂ was found to adsorb reversibly onto the (M) charge-balancing cations with formation of linear end-on adducts of the type M...OCO. Carbon dioxide also forms different carbonate-like species upon adsorption on the Na(Mg)-ETS-10, which are the origin of the activity of ETS-10 in heterogeneous base-catalyzed processes.

Gervasini et al. (2000) studied the adsorption and surface properties of Cu-exchanged ETS-10 by calorimetry of adsorbed NO, CO, C₂H₄ and NH₃ probe molecules. Cu(I) is the prominent species in Cu-ETS-10 and the number of Cu(I) species increased as the level of copper loading increases. Unfortunately, the structure of ETS-10 collapses at high copper loadings. Adsorption of several alkylamines by ETS-10 was also studied by Ruiz et al. (2004a,b), while Bagnasco et al. (2003) reported on the adsorption of water and ammonia on this material.

Serralha et al. (2000) showed that ETS-10 materials are good supports for an enzymatic alcoholysis reaction. The recombinant cutinase *Fusarium solani pisi* was immobilized by adsorption on ETS-10, ETAS-10 and vanadosilicate analogue of ETS-10, AM-6. The enzymatic activity in the alcoholysis of butyl acetate with hexanol, in isooctane, was measured as a function of the water content and water activity.

The synthesis of the pure chiral polymorph of ETS-10 would offer the potential for chiral catalysis or asymmetric synthesis. Along with zeolite beta, ETS-10 is currently the only known wide-pore microporous material which possesses a chiral polymorph with a spiral channel. The as-prepared materials of both these structures contain an equal proportion of intimately intergrown enantiomorphs and are consequently achiral. The task of preparing a pure chiral polymorph remains a formidable challenge.

Much research is now being carried out aimed at preparing zeolites membranes for applications in membrane reactors (Coronas and Santamaria 2004). Although most of the work has concentrated on "traditional" zeolites a few studies are available on microporous titanosilicate membranes, particularly on ETS-4 (Braunbarth et al. 2000a; Guan et al. 2001, 2002). The heteroepitaxial growth of ETS-10 on ETS-4 was described by Jeong et al. (2002b). Lin et al. (2004) have recently prepared a pure, 5 μm thick ETS-10 membrane exhibiting a good degree of crystal intergrowth. The development of titanosilicate-based membranes is likely to continue on account of some key advantages related to their preparation and properties, namely: (a) in general, a pure phase can be obtained in the absence of costly organic templates, thus avoiding calcination, which often leads to defects and loss of active surface groups (Dong et al. 2000); (b) titanosilicates are prepared under relatively mild pH conditions, reducing the chemical attack on the support and synthesis equipment used; (c) OPT materials present novel possibilities for isomorphous framework substitution, which allow the fine tuning of the catalytic and adsorption properties of a given membrane, while preserving its microporous structure; (d) these materials often exhibit strong basicity that provides an alternative to the acid properties of classic zeolites and opens up new application possibilities. Although ETS-10 has no natural counterpart, its catalytic properties are much studied and, thus, it is a convenient case in point. ETS-10 catalytic membrane could perform the gas-phase oxidative dehydrogenation of cyclohexanol (Valente et al. 2001) while simultaneously removing the desired product from the reaction environment. Another example would be the use of an ETS-10 membrane to catalyse the liquid-phase acylation of alcohol (Waghmode et al. 2001) and the aldol condensation of acetone (Philippou and Anderson 2000) and to remove *in situ* the product water.

Cation exchange

OPT materials present new opportunities for ion-exchange applications. Clearfield and co-workers have shown that the unique selectivity of titano- and zirconosilicates is due to the correspondence of the geometrical parameters of their ion exchange sites (channels, cavities) to the size of the selectively sorbed ions (Harrison 1995; Poojary et al. 1994; Behrens et al. 1996; Poojary et al. 1996). Because of the small size of the channels or cavities, the framework acts as a coordinating ligand to the cations.

Much attention has been focused on two structurally-related titanosilicates, $\text{Na}_2\text{Ti}_2\text{O}_3\text{SiO}_4 \cdot 2\text{H}_2\text{O}$ and synthetic pharmacosiderite, $\text{HM}_3\text{Ti}_4\text{O}_4(\text{SiO}_4)_3 \cdot 4\text{H}_2\text{O}$. The former displays great affinity for Cs^+ (Poojary et al. 1994; Bortun et al. 1996) while the latter is selective for ppm concentrations of Cs^+ and Sr^{2+} in the presence of ppm levels of Na^+ , K^+ , Mg^{2+} and Ca^{2+} cations at pH 7 (Behrens and Clearfield 1997; Behrens et al. 1998; Puziy 1998). Dyer et al. (1999) have also reported on the removal of trace ^{137}Cs and ^{89}Sr by different cationic forms of synthetic pharmacosiderite. Other recent reports on $\text{M}_2\text{Ti}_2\text{O}_3\text{SiO}_4 \cdot 2\text{H}_2\text{O}$ further show the importance of this material as a Cs^+ and Sr^{2+} exchanger (Sylvester et al. 1999; Clearfield et al. 2000; Clearfield 2001; Solbra et al. 2001) and its relevance to treat radioactive wastes containing ^{241}Am and ^{236}Pu (Al-Attar et al. 2003) and ^{134}Cs and ^{89}Sr and ^{57}Co (Moller et al. 2002).

The synthetic analogues of mineral umbite, AM-2 materials ($\text{K}_2\text{MSi}_3\text{O}_9 \cdot 2\text{H}_2\text{O}$, $M = \text{Ti}$, Zr) (Lin et al. 1999a) were shown to be good exchangers for Rb^+ , Cs^+ and K^+ cations (Bortun et al. 2000; Valtchev et al. 1999). The ion-exchange behavior of a series of mixed Zr, Ti AM-2 materials containing different amounts of Ti and Zr was studied. It was found that Zr-rich silicates with large channels exhibit affinity for Rb^+ and Cs^+ cations, whereas Ti-rich compounds with much smaller channels show a preference for the K^+ ion (Clearfield et al. 1998). These data suggest that the chemical alteration of the structure of exchangers may be a promising way for tailoring their selectivity.

The ion-exchange for uranium in microporous titanosilicates ETS-10, ETS-4, and $\text{Na}_2\text{Ti}_2\text{O}_3\text{SiO}_4 \cdot 2\text{H}_2\text{O}$ has been studied by Al-Attar et al. (2000) and Al-Attar and Dyer (2001). The difference in their ability to take up uranium has been discussed in terms of their crystal structure and the determination of their cation exchange capacity. Pavel et al. 2002 studied the sorption of ^{137}Cs and ^{60}Co by ETS-10 and ETS-4, while Al-Attar et al. 2003 examined the potential of these materials for treating radioactive wastes containing ^{241}Am and ^{236}Pu . ETS-10 was shown to be particularly selective for Pb^{2+} ions (Kuznicki and Trush 1991b; Zhao et al. 2003).

Koudsy and Dyer (2001) studied the sorption of radioactive ^{60}Co by the synthetic titanosilicate analogue of mineral penkvilsite-2O (AM-3). Synthetic penkvilsite was also shown to be particularly selective for Li^+ cations, suggesting possible applications in battery technology (Kuznicki et al. 1999).

Optical and magnetic properties

The presence of stoichiometric quantities of transition metals in the OPT frameworks may confer these materials interesting optical properties (De Man and Sauer 1996; Mihailova et al. 1996; Xu et al. 1997; Borello et al. 1997; Lamberti 1999). The structure of ETS-10 contains $-\text{O}-\text{Ti}-\text{O}-\text{Ti}-\text{O}-$ ("TiO") chains, with alternating long-short bonds, which are effectively isolated from each other by a silicate sheet. In other words, ETS-10 contains "TiO"-wires embedded in an insulating SiO_2 matrix, which leads to a one-dimensional quantum confinement of electrons or holes within this wire and a band-gap blue shift. The effective reduced mass, μ , of electrons and holes within such a wire is calculated to be

$1.66 \text{ M(e)} < \mu < 1.97 \text{ M(e)}$, which is consistent with a band gap of 4.03 eV, much different from that of bulk TiO_2 . *Ab initio* calculations on a "TiO"-chain embedded in an envelope of SiO_4 tetrahedra, mimicking the structure of ETS-10, confirm that the peculiar optical properties of solid are associated with the presence of such linear chains (Bordiga et al. 2000; Damin et al. 2004). The UV-Vis spectra and the electron spin resonance properties of the chains may be modified by adsorbing Na vapors: $\text{Ti(IV)} + \text{Na} \rightarrow \text{Ti(III)} + \text{Na}^+$, thus generating both unpaired electrons within the titanate chain, and extra cation sites. After this reduction the material is not air stable and is easily reoxidized, generating additional Na_2O within the channels. Such redox couples give strong indications of possible applications in battery technology. These studies also highlight the possible future role of OPT materials in optoelectronic and non-linear optical applications.

Lanthanide (Ln) containing materials emit over the entire spectral range: near infrared (Nd^{3+} , Er^{3+}), red (Eu^{3+} , Pr^{3+} , Sm^{3+}), green (Er^{3+} , Tb^{3+}), and blue (Tm^{3+} , Ce^{3+}). Their optical transitions take place only between 4f orbitals, which are well shielded from their chemical environment by $5s^2$ and $5p^6$ electrons (Rocha and Carlos 2003). As a consequence, atomic-like emission spectra displaying characteristic sharp lines may be observed. These materials find applications in many important devices, for example in cathode ray tubes, projection televisions, fluorescent tubes and x-ray detectors, and in photonics and optical communications.

In the last few years, much research has been carried out on materials comprising lanthanide guests in microporous zeolite-type hosts, systems which often exhibit photoluminescent properties; this field has been recently reviewed by Rocha and Carlos (2003). Microporous materials hosting lanthanide luminescent centers encompass: (a) zeolites doped via ion exchanging the extra-framework cations by Ln^{3+} ; (b) lanthanide complexes with organic ligands, enclosed in the zeolitic pores and channels; (c) open-framework coordination polymers (organic-inorganic hybrids); and (d) novel lanthanide silicates, with stoichiometric amounts of framework Ln^{3+} ions (see section on Rare-earth silicates).

ETS-10 has been doped with Eu^{3+} (Rainho et al. 2000) and Er^{3+} (Rocha et al. 2000a) by ion-exchanging the Na^+ and K^+ cations, and studied the luminescence properties of these materials. Only Eu^{3+} -doped ETS-10 is optically active, even at 300 K. However, the presence of water molecules within the channels of ETS-10, coordinating Eu^{3+} , partially quenches the radiative process, reducing photoluminescence. The emission spectrum indicates the presence of, at least, two local environments for the Eu^{3+} ions in ETS-10. Similar studies were carried out on titanosilicates AM-2 and AM-3 (Rocha et al. 2004a) and zirconosilicate analogue of AM-2 (Rainho et al. 2004). One possible way to circumvent the quenching of photoluminescence by water molecules and hydroxyl ions in these materials consists in collapsing the microporous framework into more dense structures. For example, Rocha and co-workers prepared luminescent dense materials from microporous precursors (Rainho et al. 2000, 2002; Rocha et al. 2000a). Upon calcinations at temperatures in excess of 700°C , Eu^{3+} - and Er^{3+} -doped ETS-10 transform into analogues of the mineral narsarsukite, which display very interesting luminescence properties. Er^{3+} -doped narsarsukite, in particular, exhibits a high and stable room-temperature emission in the visible and infrared spectral regions (Rocha et al. 2000a). An efficient energy transfer between the narsarsukite skeleton and the Er^{3+} centers shows that the ion-lattice interactions can play an important role in the luminescence properties of these titanosilicates.

Embedding lanthanide ions in the framework is a novel approach proposed by Rocha and co-workers for preparing photoluminescent microporous material, which contain stoichiometric amounts of Ln (Rocha and Carlos 2003). These materials are important because they are multifunctional, combining in a single, stable solid microporosity and photoluminescence. Rocha et al. (2000b) reported Ce^{3+} -monteregianite-type materials (AV-5). The Ce(III)/Ce(IV)

ratio in AV-5 may be controlled by oxidation/reduction in an appropriate atmosphere, allowing the fine tuning of the luminescence, adsorption and ion exchange properties of the material. Eu- and Tb-AV-9 monterejanite-type materials are photoluminescent in the visible region (Ananias et al. 2001) while dehydrated Er-AV-9 (Ananias et al. 2004) and Nd-AV-9 (Rocha et al. 2004a) are room-temperature infrared emitters. Tb-AV-9 is also the first example of a microporous siliceous x-ray scintillator (Ananias et al. 2004), i.e., it emits in the visible region when excited with X-ray ($\text{CuK}\alpha$) radiation (integrated intensity 60% of that of standard material $\text{Gd}_2\text{O}_3:\text{S:Tb}$). The sazhinite-type material AV-21 $[\text{Na}_3(\text{EuSi}_6\text{O}_{15})\cdot 2\text{H}_2\text{O}]$ is photoluminescent in the visible region. When excited at 394 nm, the room-temperature emission spectra of hydrated and dehydrated AV-21 exhibit subtle differences, particularly a shift in the ${}^5\text{D}_0 \rightarrow {}^7\text{F}_0$ transition lines. This observation raises the possibility of using the photoluminescence of this material to sense the presence of other molecules (Rocha et al. 2004b).

Tobermorite-like, AV-20 materials $(\text{Na}_{1.08}\text{K}_{0.5}\text{Ln}_{1.14}\text{Si}_3\text{O}_{8.5}\cdot 1.78\text{H}_2\text{O}, \text{Ln} = \text{Eu}, \text{Tb}, \text{Sm}, \text{Ce}, \text{Gd})$ have very interesting photoluminescent properties (Ferreira et al. 2003a). In particular, introducing a second type of Ln^{3+} ion in the framework allows the tuning of photoluminescence: the gathered evidence clearly shows the occurrence of energy transfer from Tb^{3+} to Eu^{3+} (in Eu/Tb-AV-20) and Gd^{3+} to Tb^{3+} (in Tb/Gd-AV-20).

Engineering the magnetic properties of OPT materials is an almost completely unexplored field with tremendous potential for applications. Some reference to the magnetic behavior (magnetic susceptibility as a function of temperature) of vanadosilicates is available from the work of Jacobson and co-workers (Wang et al. 2001, 2002c; Huang et al. 2002) and Li et al. (2002). As the valence state of vanadium can be easily manipulated novel magnetic properties may be anticipated. In practice, so far, the materials are paramagnetic down to very low temperatures (a few degrees K) when they may exhibit weak pairwise antiferromagnetic interactions. Brandão et al. (2004) reported a large-pore paramagnetic cromosilicate material (AV-15, $\text{Na}_3\text{CrSi}_6\text{O}_{15}\cdot 4\text{H}_2\text{O}$) with a pseudo-Curie temperature of 0.71 K and a magnetic moment of $3.69 \mu_B$, indicating the presence of Cr(III).

Perhaps the most interesting attempt to engineer magnetic centers in OPT materials is the synthesis by Wang et al. (2003) of the copper silicate system CuSH-1A ($A = \text{Na}, \text{K}, \text{Rb}, \text{Cs}, x \approx 1, y \approx 1, z \approx 6$): $\text{Na}_4[\text{Cu}_2\text{Si}_{12}\text{O}_{27}(\text{OH})_2][(\text{A}(\text{OH}))_x(\text{NaOH})_y(\text{H}_2\text{O})_z]$. These structures are unusual in several respects: they are the first examples to contain double layers of silicate tetrahedra that define straight 12-ring channels, analogous to those found in LTL-type zeolites. Unlike LTL, however, the framework composition $\text{Na}_4[\text{Cu}_2\text{Si}_{12}\text{O}_{27}(\text{OH})_2]$ that defines the 12-ring channels is neutral, and as a consequence only neutral MOH and H_2O species fill these channels. The porous framework is built from silicate double layers that are arranged perpendicular to the $[100]$ direction, and are cross-linked by interlayer Cu-O and Na-O bonds (Fig. 8). The silicate double layer contains channels defined by 12-rings of tetrahedra that run along the $[001]$ direction and have an aperture of $7.3 \times 4.4 \text{ \AA}^2$, and 8-ring channels along the $[011]$ and $[0\bar{1}1]$ directions, with an aperture of $3.8 \times 2.5 \text{ \AA}^2$. Neighboring silicate double layers are intercon-

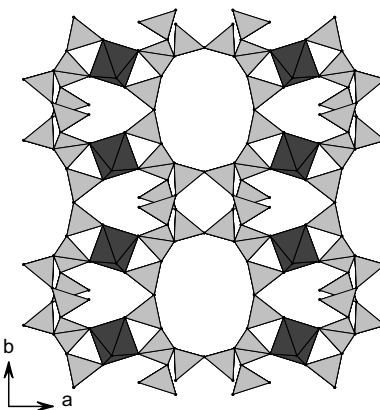


Figure 8. Structure of copper silicate CuSH-1Cs viewed along the $[001]$ direction showing the 12-ring channels. Dark CuO_6 octahedra, light grey SiO_4 tetrahedra. Na^+ , Cs^+ and water molecules are omitted for clarity.

nected by CuO_4 squares that share corners with SiO_4 tetrahedra, with Cu-O bond lengths of 1.95 Å. The copper-ion coordination is completed by interlayer water molecules to form single chains of $\text{CuO}_4(\text{H}_2\text{O})_2$ elongated octahedra with Cu-OH₂ bond lengths of 2.70 Å.

CONCLUSIONS AND OUTLOOK

The research into mixed octahedral-pentahedral-tetrahedral microporous silicates is now a well established field. The initial impetus on titanosilicates has been followed by a comprehensive synthesis effort leading to many new transition metal silicates. A few examples of calcium, tin, indium and uranium silicates have also been reported. At present, the synthesis effort is also being directed towards lanthanide silicates.

The study of OPT materials brought to light new molecular architectures and has broadened considerably our understanding of the chemistry (and, to some extent, the physics) of microporous zeolite-type materials. So far, the search for potential applications of OPT materials has been concentrated on titanosilicate ETS-10 and heterogeneous catalysis, exploring the intrinsic basic properties and photocatalytic activity of this material. An important body of work is also available on the use of small-pore OPT titanosilicates and zirconosilicates as ion-exchangers, particularly for the treatment of radioactive wastes, and in the field of adsorption and separation of small molecules.

In the near future it is anticipated that the catalysis applications will become even more important, clearly showing that the research into OPT materials is not simply an academic exercise (even if a most rewarding one). We feel, however, that perhaps the real potential of these new materials lies not in the “conventional” areas of use of zeolites but rather in totally new fields, such as optoelectronics and non-linear optics, batteries, magnetic materials, sensors and other nanotechnology device applications. The new research into photoluminescent lanthanide silicates and the very recent development of (potentially) magnetic copper silicates provides the first hints that some of the most interesting properties of OPT materials remain largely uncovered.

The expedition into the exotic world of OPT materials has been motivated, in no small measure, by the sense of wonder conveyed by the amazing mineral structures provided by Nature. Clearly, this intellectual endeavor overrides any artificial borders scientists may have built up in the past between Chemistry, Physics and Mineralogy. In this sense, the field of OPT materials also presents excellent scientific case studies for undergraduate and graduate students, no longer being in the strict possession of a number of (excited) scientists.

ACKNOWLEDGMENTS

We thank financial support from FCT, POCTI and FEDER.

REFERENCES

- Al-Attar L, Dyer A (2001) Sorption of uranium onto titanosilicate materials. *J Radioanal Nucl Chem* 247: 121-128
- Al-Attar L, Dyer A, Blackburn R (2000) Uptake of uranium on ETS-10 microporous titanosilicate. *J Radioanal Nucl Chem* 246:451-455
- Al-Attar L, Dyer A, Harjula R (2003) Uptake of radionuclides on microporous and layered ion exchange materials. *J Mater Chem* 13:2963-2968
- Ananias D, Ferreira A, Rocha J, Ferreira P, Rainho JP, Morais C, Carlos LD (2001) Novel microporous framework europium and terbium silicates. *J Am Chem Soc* 123:5735-5742

- Ananias D, Rainho JP, Ferreira A, Rocha J, Carlos LD (2004) The first examples of X-ray phosphors, and C-band infrared emitters based on microporous lanthanide silicates. *J Alloys Compd* 374:219-222
- Anderson MW, Agger JR, Hanif N, Terasaki O (2001a) Growth models in microporous materials. *Microporous Mesoporous Mater* 48:1-9
- Anderson MW, Agger JR, Hanif N, Terasaki O, Ohsuna T (2001b) Crystal growth in framework materials. *Solid State Sci* 3:809-819
- Anderson MW, Philippou A, Lin Z, Ferreira A, Rocha J (1995a) Al, Ti, avoidance in the microporous titanosaluminosilicate ETAS-10. *Angew Chem, Int Ed Engl* 34:1003-1005
- Anderson MW, Rocha J (2002) Synthesis of titanosilicates and related materials. *In: Handbook of porous solids*. Vol 2. Schüth F, Sing KSW, Weitkamp J (eds) Wiley-VCH, Weinheim, p 876-903
- Anderson MW, Terasaki O, Ohsuna T, O'Malley PJ, Philippou A, Mackay SP, Ferreira A, Rocha J, Lidin S (1995b) Microporous titanosilicate ETS-10: a structural survey. *Philos Mag B* 71:813-841
- Anderson MW, Terasaki O, Ohsuna T, Philippou A, Mackay SP, Ferreira A, Rocha J, Lidin S (1994) Structure of the microporous titanosilicate ETS-10. *Nature* 367:347-351
- Bagnasco G, Turco M, Busca G, Armaroli T, Nastro A, De Luca P (2003) Characterization of the structural and gas adsorption properties of ETS-10 molecular sieve. *Adsorpt Sci Technol* s21:683-696
- Bal R, Chaudhari K, Srinivas D, Sivasanker S, Ratnasamy P (2000) Redox and catalytic chemistry of Ti in titanosilicate molecular sieves: an EPR investigation. *J Mol Catal A: Chem* 162:199-207
- Baussy G, Caruba R, Baumer A, Turco G (1974) Experimental mineralogy in ZrO_2 - SiO_2 - Na_2O - H_2O system – petrogenetic correlations. *Bull Soc Fr Minéral Crystallogr* 97:433-444
- Behrens EA, Clearfield A (1997) Titanium silicates, $M_3HTi_4O_4(SiO_4)_3 \cdot 4H_2O$ ($M = Na^+, K^+$), with three-dimensional tunnel structures for the selective removal of strontium and cesium from wastewater solutions. *Microporous Mater* 11:65-75
- Behrens EA, Poojary DM, Clearfield A (1996) Syntheses, crystal structures, and ion-exchange properties of porous titanosilicates, $HM_3Ti_4O_4(SiO_4)_3 \cdot 4H_2O$ ($M=H^+, K^+, Cs^+$), structural analogues of the mineral pharmacosiderite. *Chem Mater* 8:1236-1244
- Behrens EA, Sylvester P, Clearfield A (1998) Assessment of a sodium nonatitanate and pharmacosiderite-type ion exchangers for strontium and cesium removal from DOE waste simulants. *Environ Sci Technol* 32:101-107
- Bianchi CL, Ardizzone S, Ragaini V (1998a) Synthesis gas to branched hydrocarbons: a comparison between Ru-based catalysts supported on ETS-10 and on Al_2O_3 (doped with sulfated zirconia). *In: Natural gas conversion V. Stud Surface Sci Catal Vol 119*. Parmaliana A, Sanfilippo D, Frusteri F, Vaccari A, Arena F (eds) Elsevier, Amsterdam, p 173-178
- Bianchi CL, Carli R, Merlotti S, Ragaini V (1996) Fischer-Tropsch synthesis on Co and Co(Ru-doped) ETS-10 titanium silicate catalysts. *Catal Lett* 41:79-82
- Bianchi CL, Ragaini V (1997) Experimental evidence of alpha-olefin readsorption in Fischer-Tropsch synthesis on ruthenium-supported ETS-10 titanium silicate catalysts. *J Catal* 168:70-74
- Bianchi CL, Vitali S, Ragaini V (1998b) Comparison between Co and Co(Ru-promoted)-ETS-10 catalysts prepared in different ways for Fischer-Tropsch synthesis. *In: Natural gas conversion V. Stud Surface Sci Catal Vol 119*. Parmaliana A, Sanfilippo D, Frusteri F, Vaccari A, Arena F (eds) Elsevier, Amsterdam, p 167-172
- Bodoardo S, Geobaldo F, Penazzi N, Arrabito M, Rivetti F, Spano G, Lamberti C, Zecchina A (2000) Voltammetric characterization of structural titanium species in zeotypes. *Electrochem Commun* 2:349-352
- Bonaccorsi E, Merlino S (2005) Modular microporous minerals: cancrinite-davyne group and C-S-H phases. *Rev Mineral Geochem* 57:241-290
- Bordiga S, Palomino GT, Zecchina A, Ranghino G, Giamello E, Lamberti C (2000) Stoichiometric and sodium-doped titanium silicate molecular sieve containing atomically defined -OTiOTiO- chains: quantum *ab initio* calculations, spectroscopic properties, and reactivity. *J Chem Phys* 112:3859-3867
- Borello E, Lamberti C, Bordiga S, Zecchina A, Arean CO (1997) Quantum-size effects in the titanosilicate molecular sieve. *Appl Phys Lett* 71:2319-2321
- Bortun AI, Bortun LN, Clearfield A (1996) Ion exchange properties of a cesium ion selective titanosilicate. *Solvent Extr Ion Exch* 14:341-354
- Bortun AI, Bortun LN, Clearfield A (1997) Hydrothermal synthesis of sodium zirconium silicates and characterization of their properties. *Chem Mater* 9:1854-1864
- Bortun AI, Bortun LN, Poojary DM, Xiang O, Clearfield A (2000) Synthesis, characterization, and ion exchange behavior of a framework potassium titanium trisilicate $K_2TiSi_3O_9 \cdot H_2O$ and its protonated phases. *Chem Mater* 12:294-305
- Brandão P, Philippou A, Hanif N, Claro PC, Rocha J, Anderson MW (2002a) Synthesis and characterization of two novel large-pore crystalline vanadosilicates. *Chem Mater* 14:1053-1057

- Brandão P, Philippou A, Rocha J, Anderson MW (2001a) Gas-phase synthesis of MTBE from methanol and t-butanol over the microporous niobium silicate AM-11. *Catal Lett* 73:59-62
- Brandão P, Philippou A, Rocha J, Anderson MW (2001b) Synthesis and characterization of chromium-substituted ETS-10. *Phys Chem Chem Phys* 1773-1777
- Brandão P, Philippou A, Rocha J, Anderson MW (2002b) Dehydration of alcohols by microporous niobium silicate AM-11. *Catal Lett* 80:99-102
- Brandão P, Valente A, Ferreira A, Amaral VS, Rocha J (2004) First stoichiometric large-pore chromium(III) silicate catalyst. *Microporous Mesoporous Mater* 69:209-215
- Brandão P, Valente A, Philippou A, Ferreira A, Anderson MW, Rocha J (2002c) Novel large-pore framework titanium silicate catalyst. *J Mater Chem* 12:3819-3822
- Brandão P, Valente A, Philippou A, Ferreira A, Anderson MW, Rocha J (2003) Hydrothermal synthesis and characterization of two novel large-pore framework vanadium silicates. *Eur J Inorg Chem* 1175-1180
- Braunbarth CM, Boudreau LC, Tsapatsis M (2000a) Synthesis of ETS-4/TiO₂ composite membranes and their pervaporation performance. *J Membr Sci* 174:31-42
- Braunbarth CM, Hillhouse HW, Nair S, Tsapatsis M, Burton A, Lobo RF, Jacobinas RM, Kuznicki SM (2000b) Structure of strontium ion-exchanged ETS-4 microporous molecular sieves. *Chem Mater* 12:1857-1865
- Calza P, Paze C, Pelizzetti E, Zecchina A (2001) Shape-selective photocatalytic transformation of phenols in an aqueous medium. *Chem Commun* 2130-2131
- Chao GY (1985) The crystal-structure of gaidonnayite Na₂ZrSi₃O₉·2H₂O. *Can Mineral* 23:11-15
- Chapman DM (1990) Crystalline group IVA metal-containing molecular sieve compositions. US Patent 5 015 453
- Chapman DM, Roe AL (1990) Synthesis, characterization and crystal-chemistry of microporous titanium-silicate materials. *Zeolites* 10:730-737
- Choisnet J, Nguyen N, Groult D, Raveau B (1976) New oxides in lattice of octahedra NbO₆ (TaO₆) and Si₂O₇ groups – phases A₃Ta₆Si₄O₂₆ (A=Ba, Sr) and K₆M₆Si₄O₂₆ (M=Nb, Ta). *Mater Res Bull* 11:887-894
- Choisnet J, Nguyen N, Groult D, Raveau B (1977) Nonstoichiometric silicotantalates and siliconiobates. *Mater Res Bull* 12:91-96
- Chukanov NV, Pekov IV (2005) Heterosilicates with tetrahedral-octahedral frameworks: mineralogical and crystal-chemical aspects. *Rev Mineral Geochem* 57:105-144
- Chukanov NV, Pekov IV, Rastsvetaeva RK (2004) Crystal chemistry, properties and synthesis of microporous silicates containing transition elements. *Russ Chem Rev* 73:227-246
- Clearfield A (2001) Structure and ion exchange properties of tunnel type titanium silicates. *Sol State Sci* 3: 103-112
- Clearfield A, Bortun LN, Bortun AI (2000) Alkali metal ion exchange by the framework titanium silicate M₂Ti₂O₃SiO₄·nH₂O (M = H, Na). *React Funct Polym* 43:85-95
- Clearfield A, Bortun LN, Bortun AI, Poojary DM, Khainakov SA (1998) On the selectivity regulation of K₂ZrSi₃O₉·H₂O-type ion exchangers. *J Mol Struct* 470:207-213
- Corcoran Jr EW, Newsam JM, King Jr HE, Vaughan DEW (1989) Phase identification of hydrothermal crystallization products from M₂O-SiO₂-SnO₂-H₂O gels or solutions. *In: Zeolite Synthesis. ACS Symposium Series #398. Occelli ML Robson HE (eds) American Chemical Society, Washington D.C., 603*
- Corcoran Jr EW, Vaughan DEW (1989) Hydrothermal synthesis of mixed octahedral-tetrahedral oxides – synthesis and characterization of sodium stannosilicates. *Solid State Ionics* 32/33:423-249
- Corcoran Jr EW, Vaughan DEW, Eberly Jr PE (1992) Stannosilicates and preparation thereof. US patent 5 110 568
- Coronas J, Santamaria J (2004) State-of-the-art in zeolite membrane reactors. *Topics Catal* 29:29-44
- Cruciani G, De Luca P, Nastro A, Pattison P (1998) Rietveld refinement of the zorite structure of ETS-4 molecular sieve. *Microporous Mesoporous Mater* 21:143-153
- Dadachov MS, Le Bail A (1997) Structure of zeolitic K₂TiSi₃O₉·H₂O determined *ab initio* from powder diffraction data. *Eur J Solid State Inorg Chem* 34:381-390
- Dadachov MS, Rocha J, Ferreira A, Anderson MW (1997) *Ab initio* structure determination of layered sodium titanium silicate containing edge-sharing titanate chains (AM-4) Na₃(Na,H)Ti₂O₂[Si₂O₆]·2.2H₂O. *Chem Commun* 2371-2372
- Damin A, Xamena FXL, Lamberti C, Civalleri B, Zicovich-Wilson CM, Zecchina A (2004) Structural, electronic, and vibrational properties of the Ti-O-Ti quantum wires in the titanosilicate ETS-10. *J Phys Chem B* 108:1328-1336
- Das TK, Chandwadkar AJ, Belhekar AA, Sivasanker S (1996a) Studies on the synthesis of ETS-10. II. Use of organic templates. *Microporous Mater* 5:401-410
- Das TK, Chandwadkar AJ, Budhkar AP, Belhekar AA, Sivasanker S (1995) Studies on the synthesis of ETS-10. I. Influence of synthesis parameters and seed content. *Microporous Mater* 4:195-203

- Das TK, Chandwadkar AJ, Sivasanker S (1996b) A rapid method of synthesizing the titanium silicate ETS-10. *Chem Commun* 1105-1106
- Das TK, Chandwadkar AJ, Sivasanker S (1998) Aromatization of n-hexane over platinum alkaline ETS-10. *In: Recent advances in basic and applied aspects of industrial catalysis. Stud Surface Sci Catal* 113. Rao TSRP, Dhar GM (ed) Elsevier, Amsterdam, p 455-462
- Das TK, Chandwadkar AJ, Soni HS, Sivasanker S (1996c) Studies on the synthesis, characterization and catalytic properties of the large pore titanosilicate, ETS-10. *J Mol Catal A: Chem* 107:199-205
- Das TK, Chandwadkar AJ, Soni HS, Sivasanker S (1997) Hydroisomerization of n-hexane over Pt-ETS-10. *Catal Lett* 44:113-117
- De Man AJM, Sauer J (1996) Coordination, structure, and vibrational spectra of titanium in silicates and zeolites in comparison with related molecules. An *ab initio* study. *J Phys Chem* 100:5025-5034
- Dong J, Lin YS, Hu MZC, Peascoe RA, Payzant EA (2000) Template-removal-associated microstructural development of porous-ceramic-supported MFI zeolite membranes. *Microporous Mesoporous Mater* 34: 241-253
- Du H, Chen J, Pang W (1996) Synthesis and characterization of a novel layered titanium silicate JDF-L1. *J Mater Chem* 6:1827-1830
- Dyer A, J  far JJ (1990) Novel stannosilicates. I. Synthesis and characterization. *J Chem Soc Dalton Trans* 3239-3242
- Dyer A, J  far JJ (1991) Novel stannosilicates. II. Cation-exchange studies. *J Chem Soc Dalton Trans* 2639-2642
- Dyer A, Pillinger M, Amin S (1999) Ion exchange of cesium and strontium on a titanosilicate analogue of the mineral pharmacosiderite. *J Mater Chem* 9:2481-2487
- Evans Jr HT (1973) Crystal-structures of cavansite and pentagonite. *Am Mineral Sect B* 58:412-424
- Ferraris G, Gula A (2005) Polysomatic aspects of microporous minerals –heterophyllosilicates, palysepioles and rhodesite-related structures. *Rev Mineral Geochem* 57:69-104
- Ferraris G, Ivaldi G, Khomyakov AP (1995) Altsite $\text{Na}_3\text{K}_6\text{Ti}_3[\text{Al}_2\text{Si}_6\text{O}_{26}]\text{Cl}_3$, a new hyperalkaline aluminosilicate from Kola Peninsula (Russia) related to lemoynite: crystal structure and thermal evolution. *Eur J Mineral* 7:537-546
- Ferreira A, Ananias D, Carlos LD, Morais CM, Rocha J (2003a) Novel microporous lanthanide silicates with tobermorite-like structure. *J Am Chem Soc* 125:14573-14579
- Ferreira A, Lin Z, Rocha J, Morais C, Lopes M, Fernandez C (2001a) *Ab initio* structure determination of a small-pore framework sodium stannosilicate. *Inorg Chem* 40:3330-3335
- Ferreira A, Lin Z, Soares MR, Rocha J (2003b) *Ab initio* structure determination of novel small-pore metal-silicates: knots-and-crosses structures. *Inorg Chim Acta* 356:19-26
- Ferreira P, Ferreira A, Rocha J, Soares MA (2001b) Synthesis and structural characterization of zirconium silicates. *Chem Mater* 13:355-363
- Fox MA, Doan KE, Dulay MT (1994) The effect of the inert support on relative photocatalytic activity in the oxidative decomposition of alcohols on irradiated titanium-dioxide composites. *Research Chem Intermediates* 20:711-722
- Francis RJ, Jacobson AJ (2001) The first organically templated open-framework niobium silicate and germanate phase: low-temperature hydrothermal syntheses of $[(\text{C}_4\text{N}_2\text{H}_{11})\text{Nb}_3\text{SiO}_{10}]$ (NSH-1) and $[(\text{C}_4\text{N}_2\text{H}_{11})\text{Nb}_3\text{GeO}_{10}]$ (NGH-1). *Angew Chem Int Ed* 40:2879-2881
- Gervasini A, Carniti P (2002) CuO_x sitting on titanium silicate (ETS-10): influence of copper loading on dispersion and redox properties in relation to de- NO_x activity. *Catal Lett* 84:235-244
- Gervasini A, Picciau C, Auroux A (2000) Characterization of copper-exchanged ZSM-5 and ETS-10 catalysts with low and high degrees of exchange. *Microporous Mesoporous Mater* 35-36:457-469
- Ghose S, Gupta PKS, Campana CF (1987) Symmetry and crystal-structure of monteregianite, $\text{Na}_4\text{K}_2\text{Y}_2\text{Si}_{16}\text{O}_{38}\cdot 10\text{H}_2\text{O}$, a double-sheet silicate with zeolitic properties. *Am Mineral* 72:365-374
- Ghose S, Wan C, Chao GY (1980) Petarosite, $\text{Na}_5\text{Zr}_2\text{Si}_6\text{O}_{18}(\text{Cl},\text{OH})\cdot 2\text{H}_2\text{O}$, a zeolite-type zirconosilicate. *Can Mineral* 18:503-509
- Guan G, Kusakabe K, Morooka S (2001) Synthesis and permeation properties of ion-exchanged ETS-4 tubular membranes. *Microporous Mesoporous Mater* 50:109-120
- Guan G, Kusakabe K, Morooka S (2002) Separation of nitrogen from oxygen using a titanosilicate membrane prepared on a porous alpha-alumina support tube. *Separ Sci Technol* 37:1031-1039
- Guan GK, Kida T, Kusakabe K, Kimura K, Fang XM, Ma TL, Abe E, Yoshida A (2004) Photocatalytic H_2 evolution under visible light irradiation on CdS/ETS-4 composite. *Chem Phys Lett* 385:319-322
- Haile SM, Wuensch BJ (2000a) Structure, phase transitions and ionic conductivity of $\text{K}_3\text{NdSi}_6\text{O}_{15}\cdot x\text{H}_2\text{O}$. I. α - $\text{K}_3\text{NdSi}_6\text{O}_{15}\cdot 2\text{H}_2\text{O}$ and its polymorphs. *Acta Crystallogr Sect B: Struct Sci* 56:335-348
- Haile SM, Wuensch BJ (2000b) Structure, phase transitions and ionic conductivity of $\text{K}_3\text{NdSi}_6\text{O}_{15}\cdot x\text{H}_2\text{O}$ -II. Structure of β - $\text{K}_3\text{NdSi}_6\text{O}_{15}$. *Acta Crystallogr Sect B: Struct Sci* 56:349-362

- Harrison WTA, Gier TE, Stucky GD (1995) Single-crystal structure of $\text{Cs}_3\text{HTi}_4\text{O}_4(\text{SiO}_4)_3 \cdot 4\text{H}_2\text{O}$, A titanosilicate pharmacosiderite analog. *Zeolites* 15:408-412
- Hesse K-F, Liebau FZ, Merlino S (1992) Crystal structure of rhodesite, $\text{HK}_{1-x}\text{Na}_{x+2y}\text{Ca}_{2-y}[\text{Si}_8\text{O}_{19}] \cdot (6-Z)\text{H}_2\text{O}$, from three localities and its relation to other silicates with dreier double layers. *Kristallogr* 199:25-48
- Howe RF, Krisnandi YK (2001) Photoreactivity of ETS-10. *Chem Commun* 1588-1589
- Huang J, Wang X, Jacobson AJ (2003) Hydrothermal synthesis and structures of the new open-framework uranyl silicates $\text{Rb}_4(\text{UO}_2)_2(\text{Si}_8\text{O}_{20})$ (USH-2Rb), $\text{Rb}_2(\text{UO}_2)(\text{Si}_2\text{O}_6) \cdot \text{H}_2\text{O}$ (USH-4Rb) and $\text{A}_2(\text{UO}_2)(\text{Si}_2\text{O}_6) \cdot 0.5\text{H}_2\text{O}$ (USH-5A; A = Rb, Cs). *J Mater Chem* 13:191-196
- Huang J, Wang XQ, Liu LM, Jacobson AJ (2002) Synthesis and characterization of an open framework vanadium silicate (VSH-16Na). *Solid State Sci* 4:1193-1198
- Hung L-I, Wang S-L, Kao H-M, Lii K-H (2003) Hydrothermal synthesis, crystal structure, and solid-state NMR spectroscopy of a new indium silicate: $\text{K}_2\text{In}(\text{OH})(\text{Si}_4\text{O}_{10})$. *Inorg Chem* 42:4057-4061
- Hung L-I, Wang S-L, Szu S-P, Hsieh C-Y, Kao H-M, Lii K-H (2004) Hydrothermal synthesis, crystal structure, solid-state NMR spectroscopy, and ionic conductivity of $\text{Na}_5\text{InSi}_4\text{O}_{12}$, a silicate containing a single 12-membered ring. *Chem Mater* 16:1660-1666
- Ilyushin GD (1993) New data on the crystal structure of umbite $\text{K}_2\text{ZrSi}_3\text{O}_9 \cdot \text{H}_2\text{O}$. *Inorg Mater* 29:853-857
- Jale SR, Ojo A, Fitch FR (1999) Synthesis of microporous zirconosilicates containing ZrO_6 octahedra and SiO_4 tetrahedra. *Chem Commun* 411-412
- Jeong H-K, Chandrasekaran A, Tsapatsis M (2002a) Synthesis of a new open framework cerium silicate and its structure determination by single crystal X-ray diffraction. *Chem Commun* 2398-2399
- Jeong H-K, Krohn J, Sujaoti K, Tsapatsis M (2002b) Oriented molecular sieve membranes by heteroepitaxial growth. *J Am Chem Soc* 124:12966-12968
- Jeong H-K, Nair S, Vogt T, Dickinson LC, Tsapatsis M (2003) A highly crystalline layered silicate with three-dimensionally microporous layers. *Nature Mater* 2:53-58
- Kampf AR, Khan AA, Baur WH (1973) Barium chloride silicate with an open framework – verplanckite. *Acta Crystallogr Sect B: Struct Sci* B29:2019-2021
- Kao H-M, Lii K-H (2002) The first observation of heteronuclear two-bond J-coupling in the solid state: Crystal structure and solid-state NMR spectroscopy of $\text{Rb}_4(\text{NbO})_2(\text{Si}_8\text{O}_{21})$. *Inorg Chem* 41:5644-5646
- Kim WJ, Kim SD, Jung HS, Hayhurst DT (2002) Compositional and kinetic studies on the crystallization of ETS-10 in the presence of various organics. *Microporous Mesoporous Mater* 56:89-100
- Kim WJ, Lee MC, Yoo JC, Hayhurst DT (2000) Study on the rapid crystallization of ETS-4 and ETS-10. *Microporous Mesoporous Mater* 41:79-88
- Koudsi UY, Dyer A (2001) Sorption of ^{60}Co on a synthetic titanosilicate analogue of the mineral penkvilksite-2O and antimonysilicate. *J Radioanal Nucl Chem* 247:209-218
- Krisnandi YK, Southon PD, Adesina AA, Howe RF (2003) ETS-10 as a photocatalyst. *Intl J Photoenergy* 5: 131-140
- Krivovichev SV, Armbruster T (2004) The crystal structure of jonesite, $\text{Ba}_2(\text{K},\text{Na})[\text{Ti}_2(\text{Si}_3\text{Al})\text{O}_{18}(\text{H}_2\text{O})](\text{H}_2\text{O})_n$: a first example of titanosilicate with porous double layers. *Am Mineral* 89:314-318
- Kuznicki SM (1989) Large-pored crystalline titanium molecular sieve zeolites. US Patent 4 853 202
- Kuznicki SM (1990) Preparation of small-pored crystalline titanium molecular sieve zeolites. US Patent 4 938 939
- Kuznicki SM, Bell VA, Nair S, Hillhouse HW, Jacobinas RM, Braunbarth CM, Toby BH, Tsapatsis M (2001) A titanosilicate molecular sieve with adjustable pores for size-selective adsorption of molecules. *Nature* 412:720-724
- Kuznicki SM, Curran JS, Yang X (1999) ETS-14 crystalline titanium silicate molecular sieves, manufacture and use thereof. US Patent 5 882 624
- Kuznicki SM, Madon RJ, Koerner GS, Thrush KA (1991) Large-pored molecular sieves and uses thereof. EPA 0405978A1
- Kuznicki SM, Thrush AK (1991a) Large-pored molecular sieves containing at least one octahedral site and tetrahedral sites of at least one type. WO91/18833
- Kuznicki SM, Thrush AK (1991b) Removal of heavy metals, especially lead, from aqueous systems containing competing ions utilizing wide-pored molecular sieves of the ETS-10 type. US Patent 4 994 191
- Kuznicki SM, Thrush AK (1993) Large-pored molecular sieves with charged octahedral titanium and charged tetrahedral aluminum sites. US Patent 5 244 650
- Lamberti C (1999) Electron-hole reduced effective mass in monoatomic ...-O-Ti-O-TiO- ... quantum wires embedded in the siliceous crystalline matrix of ETS-10. *Microporous Mesoporous Mater* 30:155-163
- Le Page Y, Perrault G (1976) Structure Cristalline de la lemoynite $(\text{Na},\text{K})_2\text{CaZr}_2\text{Si}_{10}\text{O}_{26} \cdot (5-6)\text{H}_2\text{O}$. *Can Mineral* 14:132-138
- Li C-Y, Hsieh CY, Lin H-M, Kao H-M, Lii H-K (2002) High-temperature, high pressure hydrothermal synthesis, crystal structure, and solid state NMR spectroscopy of a new vanadium(IV) silicate: $\text{Rb}_2(\text{VO})(\text{Si}_4\text{O}_{10}) \cdot x\text{H}_2\text{O}$. *Inorg Chem* 41:4206-4210

- Lin Z, Rocha J, Brandão P, Ferreira A, Esculcas AP, Pedrosa de Jesus JD, Philippou A, Anderson MW (1997) Synthesis and structural characterization of microporous umbite, penkvilksite and other titanosilicates. *J Phys Chem* 101:7114-7120
- Lin Z, Rocha J, Ferreira P, Thursfield A, Agger JR, Anderson MW (1999a) Synthesis and characterization of microporous zirconium silicates. *J Phys Chem B* 103:957-963
- Lin Z, Rocha J, Navajas A, Téllez C, Coronas J, Santamaria J (2004) Synthesis and characterization of ETS-10 membranes. *Microporous Mesoporous Mater* 67:79-86
- Lin Z, Rocha J, Pedrosa de Jesus JD, Ferreira A (2000) Synthesis and structure of novel microporous framework stannosilicate. *J Mater Chem* 10:1353-1356
- Lin Z, Rocha J, Valente A (1999b) Synthesis and characterization of a framework microporous stannosilicate. *Chem Commun* 2489-2490
- Liu X, Shang M, Thomas JK (1997a) Synthesis and structure of a novel microporous titanosilicate (UND-1) with a chemical composition of $\text{Na}_{2.7}\text{K}_{5.3}\text{Ti}_4\text{Si}_{12}\text{O}_{36}\cdot 4\text{H}_2\text{O}$. *Micropor Mater* 10:273-281
- Liu X, Thomas JK (1996) Synthesis of microporous titanosilicates ETS-10 and ETS-4 using solid TiO_2 as the source of titanium. *Chem Commun* 1435-1436
- Liu Y, Du H, Xiao F, Zhu G, Pang W (2000) Synthesis and characterization of a novel microporous titanosilicate JLU-1. *Chem Mater* 12:665-670
- Liu Y, Du H, Xu Y, Ding H, Pang W, Yue Y (1999) Synthesis and characterization of a novel microporous titanosilicate with a structure of penkvilksite-*IM*. *Microporous Mesoporous Mater* 28:511-517
- Liu Y, Du H, Zhou F, Pang W (1997b) Synthesis of a new titanosilicate: an analogue of the mineral penkvilksite. *Chem Commun* 1467-1468
- MacDonald AM, Chao GY (2004) Haineaultite, a new hydrated sodium calcium titanosilicate from Mont Saint-Hilaire, Quebec: description, structure determination and genetic implications. *Can Mineral* 42:769-780
- Maurice OD (1949) Transport and deposition of the non-sulfide vein minerals. V. Zirconium minerals. *Econ Geol* 44:721-731
- Merinov BV, Maksimov BA, Belov NV (1980) The crystal structure of sodium scandium silicate $\text{Na}_3\text{ScSi}_4\text{O}_{12}$. *Doklady Akademii Nauk SSSR* 255:577-582 (in Russian)
- Mer'kov AN, Bussen IV, Goiko EA, Kul'chitskaya EA, Men'shikov YuP, Nedorezova AP (1973) Raite and zorite, new minerals from the Lovozero tundra. *Zap Vses Mineral Obs* 102:54-62 (in Russian)
- Merlino S, Bonaccorsi E, Armbruster T (2001) The real structure of tobermorite 11 Å: normal and anomalous forms, OD character and polytypic modifications. *Eur J Mineral* 13:577-590
- Merlino S, Pasero M, Artioli G, Khomyakov AP (1994) Penkvilksite, a new kind of silicate structure – OD character, X-ray single-crystal (1M), and powder rietveld (2O) refinements of 2 MDO polytypes. *Am Mineral* 79:1185-1193
- Mihailova B, Valtchev V, Minatova S, Konstantinov L (1996) Vibrational spectra of ETS-4 and ETS-10. *Zeolites* 16:22-24
- Miraglia PQ, Yilmaz B, Warzywoda J, Bazzana S, Sacco Jr A (2004) Morphological and surface analysis of titanosilicate ETS-4 synthesized hydrothermally with organic precursors. *Microporous Mesoporous Mater* 69:71-76
- Moller T, Harjula R, Lehto J (2002) Ion exchange of ^{85}Sr , ^{134}Cs and ^{57}Co in sodium titanosilicate and the effect of crystallinity on selectivity. *Separation Purification Technol* 28:13-23
- Nair S, Jeong HK, Chandrasekaran A, Braunbarth CM, Tsapatsis M, Kuznicki SM (2001) Synthesis and structure determination of ETS-4 single crystals. *Chem Mater* 13:4247-4254
- Nyman M, Tripathi A, Parise JB, Maxwell RS, Harrison WTA, Nenoff TM (2001) A new family of octahedral molecular sieves: Sodium Ti/Zr-IV niobates. *J Am Chem Soc* 123:1529-1530
- Nyman M, Tripathi A, Parise JB, Maxwell RS, Nenoff TM (2002) Sandia octahedral molecular sieves (SOMS): Structural and property effects of charge-balancing the M-IV-substituted (M = Ti, Zr) niobate framework. *J Am Chem Soc* 124:1704-1713
- Pavel CC, Vuono D, Nastro A, Nagy JB, Bilba N (2002) Synthesis and ion exchange properties of the ETS-4 and ETS-10 microporous crystalline titanosilicates. *In: Impact of Zeolites and Other Porous Materials on the New Technologies at the Beginning of the Millennium. Studies Surface Sci Catal Vol 142 (A,B)*. Aiello R, Giordano G, Testa F (eds) Elsevier, Amsterdam, p 295-302
- Perrault PG, Boucher C, Vicat J, Cannillo E, Rossi G (1973) Crystal-structure of nenadkevichite - $(\text{Na},\text{K})_{2-x}(\text{Nb},\text{Ti})(\text{O},\text{OH})\text{Si}_2\text{O}_6\cdot 2\text{H}_2\text{O}$. *Acta Crystallogr Sect B: Struct Sci* 29:1432-1438
- Philippou A, Anderson MW (1996) Structural investigation of ETS-4. *Zeolites* 16:98-107
- Philippou A, Anderson MW (2000) Aldol-type reactions over basic microporous titanosilicate ETS-10 type catalysts. *J Catal* 189:395-400
- Philippou A, Brandão P, Ghanbari-Siakhali A, Dwyer J, Rocha J, Anderson MW (2001) Catalytic studies of the novel microporous niobium silicate AM-11. *Appl Catal A* 207:229-238

- Philippou A, Naderi M, Pervaiz N, Rocha J, Anderson MW (1998a) n-hexane reforming reactions over basic Pt-ETS-10 and Pt-ETAS-10. *J Catal* 178:174-181
- Philippou A, Naderi M, Rocha J, Anderson MW (1998b) Dehydration of t-butanol over basic ETS-10, ETAS-10 and AM-6 catalysts. *Catal Lett* 53:221-224
- Philippou A, Rocha J, Anderson MW (1999) The strong basicity of the microporous titanosilicate ETS-10. *Catal Lett* 57:151-153
- Poojary DM, Bortun AI, Bortun LN, Clearfield A (1996) Structural studies on the ion-exchanged phases of a porous titanosilicate, $\text{Na}_2\text{Ti}_2\text{O}_3\text{SiO}_4 \cdot 2\text{H}_2\text{O}$. *Inorg Chem* 35:6131-6139
- Poojary DM, Bortun AI, Bortun LN, Clearfield A (1997) Syntheses and X-ray powder structures of $\text{K}_2\text{ZrSi}_3\text{O}_9 \cdot \text{H}_2\text{O}$ and its ion-exchanged phases with Na and Cs. *Inorg Chem* 36:3072-3079
- Poojary DM, Cahill RA, Clearfield A (1994) Synthesis, crystal-structures, and ion-exchange properties of a novel porous titanosilicate. *Chem Mater* 6:2364-2368
- Puziy AM (1998) Cesium and strontium exchange by the framework potassium titanium silicate $\text{K}_2\text{HTi}_4\text{O}_4(\text{SiO}_4)_3 \cdot 4\text{H}_2\text{O}$. *J Radioanal Nucl Chem* 237:73-79
- Rainho JP, Ananias D, Lin Z, Ferreira A, Carlos LD, Rocha J (2004) Photoluminescence and local structure of Eu(III)-doped zirconium silicates. *J Alloys Compd* 374:185-189
- Rainho JP, Carlos LD, Rocha J (2000) New phosphors based on Eu^{3+} -doped microporous titanosilicates. *J Lumin* 87-89:1083-1086
- Rainho JP, Pillinger M, Carlos LD, Ribeiro SJL, Almeida RM, Rocha J (2002) Local Er(III) environment in luminescent titanosilicates prepared from microporous precursors. *J Mater Chem* 12:1162-1168
- Rastsvetaeva RK, Andrianov VI (1984) Refined crystal-structure of vinogradovite. *Sov Phys Crystallogr* 29:403-406
- Rinaldi R, Pluth JJ, Smith JV (1975) Crystal-structure of cavansite dehydrated at 220°C. *Acta Crystallogr Sect B: Struct Sci* 31:1598-1602
- Roberts MA, Sankar G, Thomas JM, Jones RH, Du H, Fang M, Chen J, Pang W, Xu R (1996) Synthesis and structure of a layered titanosilicate catalyst with five-coordinate titanium. *Nature* 381:401-404
- Rocha J, Anderson MW (2000) Microporous titanosilicates and other novel mixed octahedral-tetrahedral framework oxides. *Eur J Inorg Chem* 801-818
- Rocha J, Brandão P, Anderson MW, Ohsuna T, Terasaki O (1998a) Synthesis and characterization of microporous titano-borosilicate ETBS-10. *Chem Commun* 667-668
- Rocha J, Brandão P, Lin Z, Anderson MW, Alfredsson V, Terasaki O (1997a) The First example of a microporous framework vanadosilicate containing hexacoordinated vanadium. *Angew Chem, Int Ed Engl* 36:100-102
- Rocha J, Brandão P, Lin Z, Esculcas AP, Ferreira A, Anderson MW (1996a) Synthesis and structural studies of microporous titanium-niobium-silicates with the structure of nenadkevichite. *J Phys Chem* 100:14978-14983
- Rocha J, Brandão P, Lin Z, Kharlamov A, Anderson MW (1996b) Novel microporous titanium-niobium-silicates with the structure of nenadkevichite. *Chem Commun* 669-670
- Rocha J, Brandão P, Pedrosa de Jesus JD, Philippou A, Anderson MW (1999) Synthesis and characterization of microporous titanoniobosilicate ETNbS-10. *Chem Commun* 471-472
- Rocha J, Brandão P, Philippou A, Anderson MW (1998b) Synthesis and characterization of a novel microporous niobium silicate catalyst. *Chem Commun* 2687-2688
- Rocha J, Carlos LD (2003) Microporous materials containing lanthanide metals. *Curr Opin Solid State Mater Sci* 7:199-205
- Rocha J, Carlos LD, Ferreira A, Rainho J, Ananias D, Lin Z (2004a) Novel microporous and layered luminescent lanthanide silicates. *Mater Sci Forum* 455-456:527-531
- Rocha J, Carlos LD, Paz FAA, Ananias D, Klinowski J (2004b) Novel microporous luminescent europium(III) silicate. *In: Recent advances in the science and technology of zeolites and related materials. Studies Surface Sci Catal Vol 154 (A,B,C)* Van Steen E, Callanan LH, Claeys M (eds) Elsevier, Amsterdam, p 3028-3034
- Rocha J, Carlos LD, Rainho JP, Lin Z, Ferreira P, Almeida RM (2000a) Photoluminescence of new Er^{3+} -doped titanosilicate materials. *J Mater Chem* 10:1371-1375
- Rocha J, Ferreira A, Lin Z, Agger JR, Anderson MW (1998c) Synthesis and characterization of a microporous zirconium silicate with the structure of petarasite. *Chem Commun* 1269-1270
- Rocha J, Ferreira A, Lin Z, Anderson MW (1998d) Synthesis of microporous titanosilicate ETS-10 from TiCl_3 and TiO_2 : A comprehensive study. *Microporous Mesoporous Mater* 23:253-263
- Rocha J, Ferreira P, Carlos LD, Ferreira A (2000b) The first microporous framework cerium silicate. *Angew Chem Int Ed* 39:3276-3279
- Rocha J, Ferreira P, Lin Z, Brandão P, Ferreira A, Pedrosa de Jesus JD (1997b) The first synthetic microporous yttrium silicate containing framework sodium ions. *Chem Commun* 2103-2104

- Rocha J, Ferreira P, Lin Z, Brandão P, Ferreira A, Pedrosa de Jesus JD (1998e) Synthesis and characterization of microporous yttrium and calcium silicates. *J Phys Chem* 102:4739-4744
- Rocha J, Lin Z, Ferreira A, Anderson MW (1995) Ga, Ti avoidance in the microporous titanogallosilicate ETGS-10. *J Chem Soc Chem Commun* 867-868
- Ruiz JAC, Ruiz VSO, Airolidi C, Pastore HO (2004a) Thermochemistry of n-alkylamines interaction with ETS-10 titaniunsilicate. *Thermochim Acta* 411:133-138
- Ruiz JAC, Ruiz VSO, Airolidi C, Pastore HO (2004b) Total acidity calculation for ETS-10 by calorimetry, thermogravimetry and elemental analysis. *Appl Catal A-General* 261:87-90
- Sandomirskii PA, Belov NV (1979) The OD structure of zorite. *Sov Phys Crystallogr* 24:686-693
- Sankar G, Bell RG, Thomas JM, Anderson MW, Wright PA, Rocha J, Ferreira A (1996) Determination of the structure of distorted TiO₆ units in the titanosilicate ETS-10 by a combination of X-ray absorption spectroscopy and computer modeling. *J Phys Chem* 100:449-452
- Serralha FN, Lopes JM, Lemos F, Prazeres DMF, Aires-Barros MR, Rocha J, Cabral JMS, Ramôa Ribeiro F (2000) Titanosilicates as supports for an enzymatic alcoholysis reaction. *React Kinet Catal Lett* 69: 217-222
- Shumyatskaya NG, Voronkov AA, Pyatenko YA (1980) Sazhinite Na₂Ge[Si₆O₁₄(OH)]·nH₂O: a new representative of the dalyite family in crystal chemistry. *Sov Phys Crystallogr* 25:419-423
- Smith JV (1988) Topochemistry of zeolites and related materials. I. Topology and geometry. *Chem Rev* 88: 149-182
- Solbra S, Alison N, Waite S, Mikhailovsky SV, Bortun AI, Bortun LN, Clearfield A (2001) Cesium and strontium ion exchange on the framework titanium silicate M₂Ti₂O₃SiO₄·nH₂O (M = H, Na). *Environ Sci Technol* 35:626-629
- Southon PD, Howe RF (2002) Spectroscopic studies of disorder in the microporous titanosilicate ETS-10. *Chem Mater* 14:4209-4218
- Suib SL (1998) Microporous manganese oxides. *Curr Opin Solid State Mater Sci* 3:63-70
- Suppes GJ, Dasari MA, Doscocil EJ, Mankidy PJ, Goff MJ (2004) Transesterification of soybean oil with zeolite and metal catalysts. *Appl Catal A-General* 257:213-223
- Sylvester P, Behrens EA, Graziano GM, Clearfield A (1999) An assessment of inorganic ion-exchange materials for the removal of strontium from simulated Hanford tank wastes. *Sep Sci Technol* 34:1981-1992
- Tsapatsis M (2002) Molecular sieves in the nanotechnology era. *AIChE Journal* 48:654-660
- Uma S, Rodrigues S, Martyanov IN, Klabunde KJ (2004) Exploration of photocatalytic activities of titanosilicate ETS-10 and transition metal incorporated ETS-10. *Microporous Mesoporous Mater* 67: 181-187
- Valente A, Lin Z, Brandão P, Portugal I, Anderson MW, Rocha J (2001) Gas phase oxidative dehydrogenation of cyclohexanol over ETS-10 and related materials. *J Catal* 200:99-105
- Valtchev V, Mintova S (1994) Synthesis of titanium silicate ETS-10 – the effect of tetramethylammonium on the crystallization kinetics. *Zeolites* 14:697-700
- Valtchev V, Paillaud J-L, Mintova S, Kessler H (1999) Investigation of the ion-exchanged forms of the microporous titanosilicate K₂TiSi₃O₉·H₂O. *Microporous Mesoporous Mater* 32:287-296
- Valtchev VP (1994) Influence of different organic-bases on the crystallization of titanium silicates ETS-10. *J Chem Soc Chem Commun* 261-262
- Waghmode SB, Das TK, Vetrivel R, Sivasanker S (1999) Influence of the nature of the exchanged ion on n-hexane aromatization activity of Pt-M-ETS-10: *Ab initio* calculations on the location of Pt. *J Catal* 185: 265-271
- Waghmode SB, Thakur VV, Sudalai A, Sivasanker S (2001) Efficient liquid phase acylation of alcohols over basic ETS-10 molecular sieves. *Tetra Lett* 42:3145-3147
- Waghmode SB, Waghlikar SG, Sivasanker S (2003) Heck reaction over Pd-loaded ETS-10 molecular sieve. *Bull Chem Soc Japan* 76:1989-1992
- Wang X, Huang J, Liu L, Jacobson AJ (2002a) The novel open-framework uranium silicates Na₂(UO₂)(Si₄O₁₀)·2.1H₂O (USH-1) and RbNa(UO₂)(Si₂O₆)·H₂O (USH-3). *J Mater Chem* 12:406-410
- Wang X, Huang J, Liu L, Jacobson AJ (2002b) [(CH₃)₄N][[(C₅H₅NH)_{0.8}(CH₃)₃(NH)_{0.2}]U₂Si₉O₂₃F₄ (USH-8): An organically templated open-framework uranium silicate. *J Am Chem Soc* 124:15190-15191
- Wang XQ, Jacobson AJ (1999) Crystal structure of the microporous titanosilicate ETS-10 refined from single crystal X-ray diffraction data. *Chem Commun* 973-974
- Wang XQ, Liu LM, Jacobson AJ (2001) The novel open-framework vanadium silicates K₂(VO)(Si₄O₁₀)·H₂O (VSH-1) and Cs₂(VO)(Si₄O₁₀)·H₂O (VSH-2). *Angew Chem Int Ed* 40:2174-2176
- Wang XQ, Liu LM, Jacobson AJ (2002e) Open-framework and microporous vanadium silicates. *J Am Chem Soc* 124:7812-7820
- Wang XQ, Liu LM, Jacobson AJ (2003) Nanoporous copper silicates with one-dimensional 12-ring channel system. *Angew Chem Int Ed* 42:2044-2047

- Xamena FXLI, Calza P, Lamberti C, Prestipino C, Damin A, Bordiga S, Pellizzetti E, Zecchina A (2003) Enhancement of the ETS-10 titanasilicate activity in the shape-selective photocatalytic degradation of large aromatic molecules by controlled defect production. *J Am Chem Soc* 125:2264-2271
- Xamena FXLI, Zecchina A (2002) FTIR spectroscopy of carbon dioxide adsorbed on sodium- and magnesium-exchanged ETS-10 molecular sieves. *Phys Chem Chem Phys* 4:1978-1982
- Xu H, Zhang YP, Navrotsky A (2001) Enthalpies of formation of microporous titanosilicates ETS-4 and ETS-10. *Microporous Mesoporous Mater* 47:285-291
- Xu Y, Ching WY, Gu ZQ (1997) Electronic structure of microporous titanasilicate ETS-10. *Ferroelectrics* 194: 219-226
- Yang X, Paillaud JL, Breukelen HFWJ, Kessler H, Duprey E (2001) Synthesis of microporous titanasilicate ETS-10 with TiF_4 or TiO_2 . *Microporous Mesoporous Mater* 46:1-11
- Zecchina A, Xamena FXLI, Paze C, Palomino GT, Bordiga S, Arean CO (2001) Alkyne polymerization on the titanasilicate molecular sieve ETS-10. *Phys Chem Chem Phys* 3:1228-1231
- Zhao GXS, Lee JL, Chia PA (2003) Unusual adsorption properties of microporous titanasilicate ETS-10 toward heavy metal lead. *Langmuir* 19:1977-1979